SANDIA REPORT

SAND97-8221 • UC–402
Unlimited Release
Printed January 1997

SERDP: Atmospheric Remote Sensing and Assessment Program — Final Report Part 1: The Lower Atmosphere

Tim P. Tooman, editor

Prepared by
Sandia National Laboratories
Albuquerque, New Mexico 87185 and Livermore, California 94551
for the United States Department of Energy
under Contract DE-AC04-94AL85000

Issued by Sandia National Laboratories, operated for the United States Department of Energy by Sandia Corporation.

Available to DOE and DOE contractors from:

Office of Scientific and Technical Information
P.O. Box 62
Oak Ridge TN 37831

Prices available from (615) 576-8401, FTS 626-8401.

Available to the public from:

National Technical Information Service
U.S. Department of Commerce
5285 Port Royal Rd.
Springfield, VA 22161

SAND97-8221 UC-402
Unlimited Release
Printed January 1997

Strategic Environmental Research and Development Program: Atmospheric Remote Sensing and Assessment Program — Final Report Part 1: The Lower Atmosphere

Tim P. Tooman, editor
Exploratory Systems Technology Department
Sandia National Laboratories
Livermore, California 94550

Abstract

This report documents work done between FY91 and FY95 for the lower atmospheric portion of the joint Department of Defense (DoD) and Department of Energy (DOE) Atmospheric Remote Sensing and Assessment Program (ARSAP) within the Strategic Environmental Research and Development Program (SERDP)[1]. The work focused on (1) developing new measurement capabilities and (2) measuring atmospheric heating in a well-defined layer and then relating it to cloud properties and water vapor content. Seven new instruments were developed for use with Unmanned Aerospace Vehicles (UAVs) as the host platform for flux, radiance, cloud, and water vapor measurements. Four major field campaigns were undertaken to use these new as well as existing instruments to make critically needed atmospheric measurements. Scientific results include the profiling of clear sky fluxes from near surface to 14 km and the strong indication of cloudy atmosphere absorption of solar radiation considerably greater than predicted by extant models.

---

[1] The work described in this report was performed under the Work for Others agreement numbered 81930121 and titled "Atmospheric Remote Sensing for the Strategic Environmental Research and Development Program (SERDP)."

Acknowledgments

The editor thanks for following people for their contributions to this document:

Will Bolton of Sandia National Laboratories for text describing the clear and cloudy sky campaigns,

Roger Busbee of Sandia National Laboratories for text and figures describing the telemetry system,

Peter Daum of Brookhaven National Laboratory for text and figures describing the Frost Point Hygrometer and the Laser Diode Hygrometer,

Sue Havre of Pacific Northwest National Laboratory for text and figures describing on site and post flight data management,

Peter LaDelfe of Los Alamos National Laboratory for text and figures describing the HONER instrument,

Gary Phipps of Sandia National Laboratory for text and figures describing the MPIR instrument,

Hank Revercomb of the University of Wisconsin for text and figures describing the UAV AERI instrument,

Graeme Stephens of Colorado State University for text and figures describing the SSP instrument,

John Vitko of Sandia National Laboratory for text describing the project transition,

Paul Weber of Los Alamos National Laboratory for text and figures describing the calibration facility, and

Ron Wurtz of Lawrence Livermore National Laboratory for text and figures describing the CDL instrument.

Contents

Figures

Tables

Chapter

1

Executive Summary

The Atmospheric Remote Sensing and Assessment Program (ARSAP) is a Department of Defense (DOD) and Department of Energy (DOE) joint program within the Strategic Environmental Research and Development Program (SERDP) Global Environmental Change thrust area. ARSAP was funded from FY91 through FY95 to develop improved measurements and understanding of the Earth's atmosphere. The program naturally divided into the study of the troposphere by the DOE and stratosphere and mesosphere by DOD. This report covers the DOE program activities, which were aimed at reducing the uncertainties associated with current knowledge of radiation cloud interactions and understanding how these uncertainties influence our ability to predict the effects of changing concentrations of greenhouse gases in the atmosphere.

The DOE effort had two major components: (1) the development of new measurement capabilities and, with this, (2) the measurement of atmospheric heating in a well defined layer and then relating it to cloud properties and water vapor content. Guidance was provided by a specially formed science team comprised of leading atmospheric scientists from ten universities and government research centers.

The DOE program focused on the Unmanned Aerospace Vehicle (UAV) as the platform of choice for atmospheric measurements from within the atmosphere. UAV's represent a rapidly expanding technology that promises both the altitude (>20 km) and endurance (>24 hr on station) desired for this kind of research. Seven new UAV compatible instruments were developed to extend flux, radiance, and cloud measurement capabilities and seven more existing instrument types were adapted to the UAV payload environment. The new instruments were (1) the Cloud Detection Lidar by Lawrence Livermore Laboratory, (2) the UAV Atmospheric Emitted Radiance Interferometer by the University of Wisconsin, (3) the Hemispheric Optimized Net Radiometer by Los Alamos National Laboratory, (4) the Multispectral Pushbroom Imaging Radiometer by Sandia National Laboratories, (5 and 6) the frost point and laser diode hygrometers by Brookhaven National Laboratory, and (7) Scanning Spectral Polarimeter by Colorado State University.

In cooperation with the DOE Atmospheric Radiation Measurement (ARM) program, four major field campaigns were undertaken to make critically

needed atmospheric measurements. During the course of these campaigns techniques for using UAVs in conjunction with manned aircraft were developed while utilizing many of the new instruments. The three to six week campaigns were flown over the Cloud and Atmospheric Radiation Testbed (CART) Site in north central Oklahoma in April 1994, October 1995, April 1996, and September 1996. Key scientific results include the profiling of clear sky fluxes from near surface to 14 km in altitude with unprecedented accuracy and the strong indication of cloudy atmosphere absorption of solar radiation as much as 50% greater than that predicted by the best extant models. Key technical accomplishments include the first ever use of UAVs for atmospheric research, the flight of UAVs in civilian airspace without chase, precision stacked flight with manned aircraft and a UAV maintaining lateral separation of a few hundred meters with vertical separations of 10 km, and a diurnal UAV mission with greater than 24 continuous hours on station without refueling.

Chapter 2

Introduction and Background

Participants

ARSAP was a multi-laboratory program jointly led by Sandia National Laboratories for the DOE and the Naval Research Laboratory for DOD. This report covers only the DOE effort.

Led by Sandia, DOE national laboratory participation included Los Alamos, Pacific Northwest, Lawrence Livermore, and Brookhaven. A strong partnership with the NASA laboratories and centers was also maintained. University scientists participated in ARSAP as scientific co-investigators and grantees. Finally, high technology aerospace companies contributed to the program, primarily by furnishing unmanned aerospace vehicles (UAVs) for carrying developed instruments and payloads.

Problem Statement

The goal of the ARSAP program was to develop improved measurements and understanding of the Earth's atmosphere and its response to global change based upon unique DOD and DOE technologies. The DOE role focused on the uncertainties associated with current knowledge of radiation cloud interactions and how these uncertainties influence our ability to understand the effects of increasing concentrations of greenhouse gases in the atmosphere. This programmatic role is responsive to DOE's mission to understand the impacts of energy policy on the environment and to DOD interest in clouds and weather as they affect military operations.

Technical Objectives

The technical objective of the lower atmosphere portion of the ARSAP program was to develop and apply improved measurement techniques to significantly reduce our uncertainty in understanding radiation-cloud interactions. These techniques involve the measurement of atmospheric heating in a well defined layer and then relating this measurement to the cloud properties and water vapor contained in the layer. This allows the testing and refining of the models that predict atmospheric heating based on such parameters.

The required measurements at the boundaries of the defined layer include upwelling and downwelling solar and thermal fluxes at both the upper and the lower surfaces. The properties of clouds within the layer that must be measured include reflectivity, ice/water phase, and droplet or crystal size. In addition, since water vapor plays a major role in radiative processes, its profile through the layer must also be measured. Each of these measurements must be made for multiple days for differing layers, including some that extend upwards in altitude to the tropopause (14 km in the mid-latitudes and 20 km in the tropics). They must also be of extremely high accuracy since the radiative, cloud, and water vapor heating effects are 10 to 25 times larger than the added atmospheric heating associated with a doubling of CO_2 (4 W/m^2), the most notorious of the greenhouse gases.

Thus the DOE objective was (1) to develop these high accuracy measurements techniques, (2) to use them to make sustained measurements up to the tropopause, and (3) to use these measurements to calibrate existing satellites and their data products to the accuracy required for climate measurements, thereby leveraging this national resource.

Technical Approach

As discussed above, certain key quantities must be measured in the atmosphere. These quantities include the solar and thermal fluxes at various levels in the troposphere, and especially at the tropopause; properties of cloud tops and layered clouds; and the distribution of upper tropospheric water vapor. Furthermore these measurements must be made up to the top of the lower layer of the atmosphere which governs our climate and for multiple days so as to sample diurnal and synoptic effects. This means multi-day measurements at altitudes up to 20 km (the tropical tropopause) are needed. These combined altitude and endurance requirements are beyond the capability of manned aircraft and are best met using the UAVs that are now under development by industry.

The approach was, first, to draw on DOE and DOD related defense technology to develop improved instruments that can both meet the measurement requirements and are also UAV compatible, i.e., compact, lightweight, and capable of fully autonomous operation. Second, the approach required flying these instruments on UAVs provided by industry, to develop and demonstrate the necessary measurement techniques and to obtain early scientific results. These early results were then integrated with related Atmospheric Radiation Measurement (ARM) measurements and Computer Hardware, Applied Mathematics, and Model Physics (CHAMMP) modeling efforts for the development of improved climate models.

A three phased approach was instituted for implementation, taking maximum advantage of the increasing instrument and UAV capabilities as they were developed by ARSAP and by industry. The first phase concentrated on demonstrating the needed accuracy in radiative flux profiling using a low altitude UAV under clear sky conditions. This phase was completed in a highly successful series of flights in April, 1994, and constituted the first ever climate measurements from a UAV. The second phase then extended these measurements to midaltitudes (14 km — the midlatitude tropopause) and to cloudy skies. This phase completed with the September, 1996, measurement campaign which included a 26 hour UAV endurance flight The third and final phase was to provide the full altitude capability (20 km — the tropical tropopause) needed for the tropics and was to have added the ability to profile upper tropospheric water vapor. Although the water vapor instrument has been developed, the tropical flight campaign was eliminated due to funding and schedule curtailment.

An element of technical and schedule risk was introduced into the program by relying on industry to develop the high altitude long endurance UAVs. This risk was mitigated by phasing the implementation as just described and by working with two separate companies, both of which were independently developing UAVs that provided the needed capabilities.

Chapter

3

Instrument Development

Introduction

A major portion of ARSAP involves the adaptation of existing DOE technology into a range of new, UAV compatible instruments for the measurement of cloud properties, radiation, and water vapor from within the atmosphere. This section discusses the motivation for the development of six new instruments, describes each in detail, and discusses a calibration facility developed for their calibration.

Cloud Properties

The optical properties of clouds govern the radiative transfer within and through them, and understanding this transfer is a key element in being able to understand the effects of clouds on climate and any buildup of greenhouse gases in the atmosphere. Optical properties can also be used to infer state parameters that are necessary for radiative modeling such as droplet size, phase (ice or water), and total water or ice content. Often in the past cloud optical properties have been derived from global scans from satellite platforms, a technique that suffers resolution, band selection, and calibration difficulties when applied to the task of retrieving these key properties.

The ARM-UAV program has funded the development of three instruments to accurately measure cloud morphology, optical depth, and radiances within the atmosphere from UAVs. The Cloud Detection Lidar (CDL) detects clouds, including subvisible cirrus, and aerosols by the back scattering of 1.053 μm laser light. The Scanning Spectral Polarimeter (SSP) is a third generation radiometer which utilizes a circular variable filter to measure solar radiation in the spectral region from 400 nm through 4000 nm with half bandwidths between 17 nm to 60 nm. Finally, the Multispectral Pushbroom Imaging Radiometer (MPIR) is a well calibrated imaging radiometer for measuring optical data in nine spectral bands ranging from the visible to 11 μm.

Cloud Detection Lidar (CDL)

Overview

The Cloud Detection Lidar (CDL) is a lidar (Light Detection And Ranging - a laser radar) built by Lawrence Livermore National Laboratory. It detects clouds and aerosols by their scattering signature. The return time from a pulsed 1.053 μm laser gives the range to the target while the amplitude of the return signal provides information on the cloud and aerosol density or ground albedo.

This system was developed to be a particularly compact and ruggedized, fully eye-safe, high performance backscatter lidar for use on high altitude (20 km) UAV platforms. The primary function of the CDL is the detection and profiling of high altitude thin cirrus clouds. It is designed to profile out to 20 km with a selectable range resolution down to 50 meters. Its ability to detect sub-visual cirrus clouds is particularly significant, since these clouds are extremely difficult to detect by other means, and can cause significant errors in the radiometric measurements.

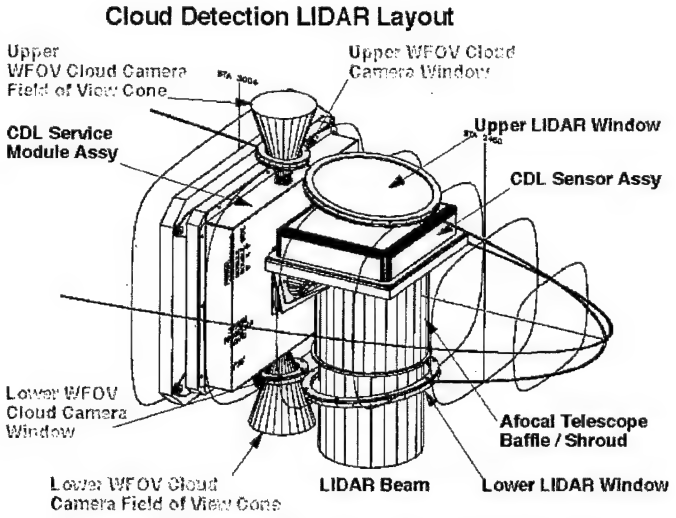

• Figure 1. Schematic of the Cloud Detection Lidar.

There are a variety of secondary goals, mostly involving determinations of cloud structure.

The lidar uses a common aperture 20 cm diameter telescope to output the transmitter beam and receive the back-scattered radiation. The system is made eye-safe through a novel approach of operating with rapid but very low energy pulses expanded over the aperture of the telescope. The system is designed to autonomously provide a single measurement each second that is calculated from the returns from 5000 separate shots to enhance the effective signal to noise. This approach, in effect, samples the profile with nearly 300 mJ of energy while maintaining the much lower (eye-safe) energy per pulse output. The lidar can be rotated to perform cloud detection either above or below the aircraft. Figure 1 shows a schematic of the instrument mounted in the nose of an airframe.

There are two wide field of view (WFOV) charge coupled device (CCD) cameras in the CDL package. These are used to provide photographic documentation of the extent of cloud cover and some information on the type and variety of ground cover. The camera images can be used to estimate fraction of cloud cover when interpreting the radiometric measurements. The CDL data and camera images can be combined to provide valuable information on the three-dimensional structure of clouds. Figure 2 shows typical CDL data taken while descending through a cirrus cloud. Data on the left hand side was taken with the instrument pointing downward; when the descent reached the middle of the cloudy layer the instrument was rotated to point upward. The color scale indicates optical density.

The CDL weighs 28 kg, consumes less than 100 watts of power, and occupies less than 0.1 cubic meter of volume. The instrument package includes the up and down looking CCD cameras which share power, control, and data lines with the CDL. The main sensor assembly contains a laser diode-pumped Nd:YLF laser with an output wavelength of 1.053 μm and operating at 5 kHz rep. rate with Q-switched 20 ns long pulses of 48 μJ/pulse. A photon counting Geiger-mode avalanche photodiode (APD) detector is used to detect the return signal. A stacked narrow bandpass interference filter and etalon combination generate a 0.1 nm wide filter with over 35% in-band transmission.

Housekeeping sensors are used for interlocks for personnel and instrument safety. Some sensors are useful for monitoring instrument status.

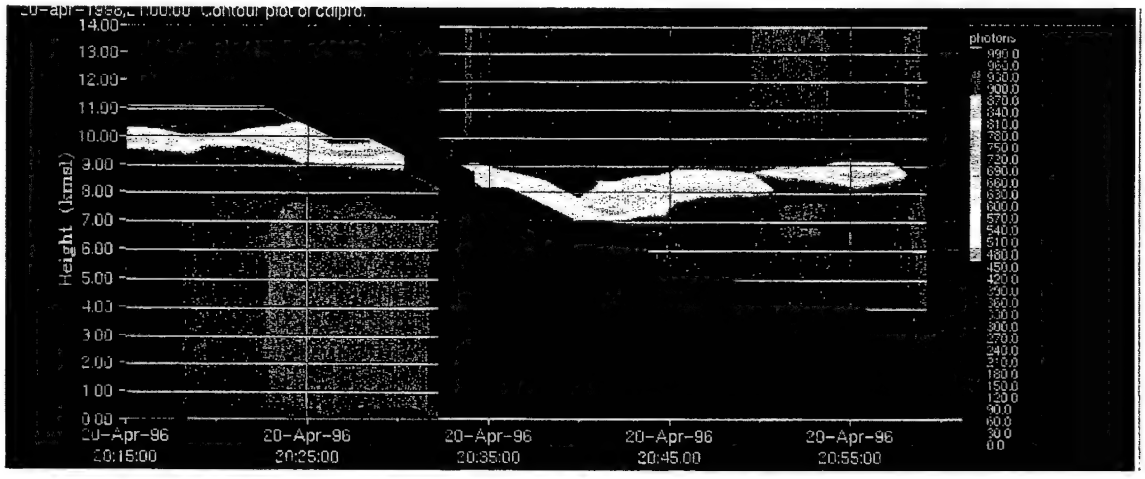

Figure 2. April 20, 1996 CDL data taken during descent through a cirrus cloud.

CDL Technical Data:

Output energy	48 μJ per pulse (CDL-L11)
Wavelength	1.053 μm
Pulse length	20 nsec
Repetition rate	5 kHz (adjustable to slower)
Output aperture	20 cm
Beam divergence	79 μrad (CDL-L11)
Beam offset (nadir)	5 +/- 0.8° forward of nadir
Beam offset (zenith)	3 +/- 0.8° forward of zenith
Detector FOV	100 μrad
Detector linearity	1.0 (linear) to 1e6 counts/sec
System sensitivity	0.0030 counts/photon (CDL-L11)
Bin boundary	no lost or double-counted counts

CDL Utilization Data:

μbin (microbin) — Fundamental unit of range measurement
width = 49.956 m
Errors (range, not rms):
+/- 0.005 m due to thermal drift of clock
+/- 0.005 m due to variation in index of refraction
+/- 0.002 m due to jitter in timing

Bin_width — User-selected integral number of μbins (2 nominal)

Range bin width - 50 m × bin_width (100 m nominal)

Range - 200 × range bin width (20 km nominal)

Range offset - 0 to 15 m (due to timing jitter in laser firing)

Sensitivity - Noise limited to sub-visual opacity of less than 0.03 (exact value depends on cloud geometry)

CDL Housekeeping Data:

Temperatures	8 sensors are monitored, 0.48°/bit
Pressure	Converted to kPa, 0.39 kPa/bit
Rotary stage position	Indicates up or down position, 1.42°/bit
Motor Current	Non-zero when rotating CDL, 3.9 mA/bit
Power Supply Current	Verifies laser power supply on, 0.039 A/bit

WFOV:

There are two WFOV cameras, one mounted to look down and one to look up. Only one camera can be operational at a time. The camera gives a black and white image 256 pixels square. Each pixel has a width/height aspect ratio of 19.6/16, where *width* corresponds to width in standard displays of imagery. The flight path is in width direction.

Camera output is 8 bits. Gain, offset and exposure time are set automatically. Exposure time can vary from 0.5 μs to 20 ms. Its sensitivity is 2 lux at f/1.2 and its spectral response is from 350 nm to 1150 nm, peaked at 650 nm, with half-peak points at 420 nm and 830 nm.

The lens is 8mm f/1.2. Pixels are 19.6 μm wide and 16.0 μm high, giving a central instantaneous field of view of 2.04 × 1.67 mrad/pixel and 24.1° × 29.3° for the entire 256 × 256 array.

Present optical design does not give overlapping images for typical UAV air speeds and altitude. Image overlap is obtained for strong headwinds.

Image is taken every 65.5 seconds. Whether images overlap to form a continuous strip depends on the speed of the UAV relative to the scene viewed and the distance to the scene. The shutter speed freezes apparent cloud scene or ground motion.

Since the cameras are intended to provide qualitative information, they have automatic gain control in order to provide the most useful images. Absolute radiance calibration is not possible.

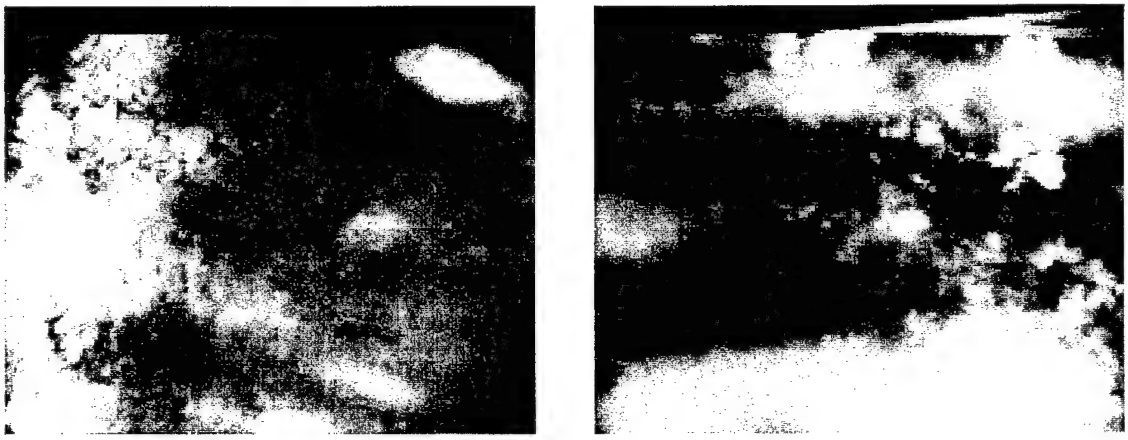

• Figure 3. Here is some data from the Wide Field of View (WFOV) camera, which is an ordinary broadband visible light camera peaking at 650nm and co-aligned with the CDL. The camera's function is to provide qualitative information on the presence, geometry, and extent of clouds. The two images contain patchy clouds at two heights. These two images are in good agreement with the CDL data which show two levels of clouds. The direction of flight of the aircraft is to the right. The field of view is 35.9 degrees in X (8 km on the ground in the first image and 7 km in the second) and 29.3 degrees in Y. The gray scale has been equalized for this report.

Scanning Spectral Polarimeter (SSP)

Purpose and Rationale

Characterizing the spectral distribution of solar radiation in the Earth's atmosphere is fundamental to understanding climate and global change for at least two reasons. Spectral reflection of sunlight from the atmosphere, and from clouds in particular, contains information about the microphysical properties of the scatterers. Second, solar radiation absorption in the atmosphere and at the surface is an important source of energy that drives the circulation of the atmosphere and oceans.

Recently our ability to model the transfer of solar radiation in the atmosphere has been called into question. The basis for doubt revolves around the long-standing question of how much absorption of solar radiation occurs in the atmosphere either under clear sky conditions or under cloudy skies. Inferred differences between measured and calculated absorptions suggest that the atmosphere absorbs much more solar radiation than is estimated from theory. Whether this increased absorption really occurs in the atmosphere and what unresolved mechanisms might produce these absorptions cannot be fully addressed without highly resolved spectral measurements of solar fluxes.

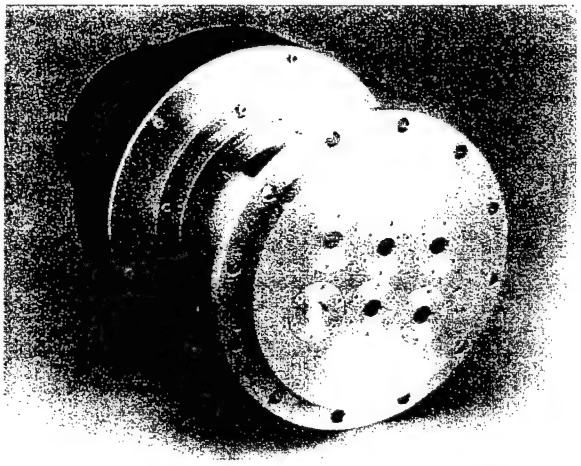

• Figure 4. SSP1

Instrument and Characteristics

These issues provide the motivation for the development of the Colorado State University Scanning Spectral Polarimeter (SSP). It is a third generation radiometer which utilizes a circular variable filter to measure solar radiation in the spectral region from 400 nm through 4000 nm with full Half Bandwidths (HBW) of less than 17 nm to 60 nm. Earlier versions of this instrument were used to measure reflectance of low level clouds. The instrument has evolved in two stages. The first stage is a version with a spectral response from 0.4-1.1 μm, referred to as the SSP1, and the second is the SSP2 with a spectral response extended to 4.0 μm. SSP1 is

fully operational and has flown on several of the campaigns described later in this report. SSP2 is currently developed and going through final tests. A feature of the SSP radiometers is that the optics are designed to be modular and possess multiple channels to provide multiple capabilities. The optical configuration of each channel can be readily changed to alter the design and performance of the instrument.

The instrument currently has six channels, five that measure spectral radiances, four of which are devoted to measurement of linear and circular polarization, and the sixth channel that measures spectral flux (Figure 4 shows the instrument and the six windows corresponding to the six channels). The instrument is much more compact than its predecessor having flown as part of the ARM UAV payload. The SSP1 version has been calibrated from 0.4 μm to 1.1 μm and is fully characterized.

Figure 5 highlights certain of these characteristics showing an example of the field of view of the radiance channels. Results are shown for one of the spectral channels and alternatively presented as a function of wavelength where the latter shows the half view angle based on a Gaussian fit of instrument output as a function of movement of a source across the FOV. A further example of the instrument characterization is given in Figure 6 (bottom) showing the bandpasses of several of the spectral channels of the SSP1.

In addition to its spectral radiance channels, the SSP1 has a channel to measure the spectral flux. This channel has a diffuser at its aperture, so as to minimize its sensitivity to the angle of the incident radiation. The top diagram in Figure 6 is the cosine response of this diffuser for selected wavelengths. These data are from analyses provided by the radiometric calibration facility at the Los Alamos National Laboratory. Generally the diffuser used has adequate cosine response except for the spectral region beyond about 0.9 μm where forward transmission peaks are observed. While these effects are removed through calibration in principle in practice a careful assessment of the nature of the diffuse cosine response is required to understand the SSP1.

Further details and examples of applications can be found at the SSP web site http://optical.atmos.colostate.edu. All electrical, mechanical, and optical characteristics are found there. The web site also includes more measurements from the SSP1 and SSP2 than are now presented.

The SSP2 is an upgraded version of the SSP1 with extended wavelength range from 0.4 μm to 4.0 μm but of the same physical dimensions as the SSP1. This instrument has been considerably miniaturized with a change in the optical configuration from that of the SSP1. A block diagram of the instrument `system' is shown in Figure 7. The instrument is currently in final stages of testing.

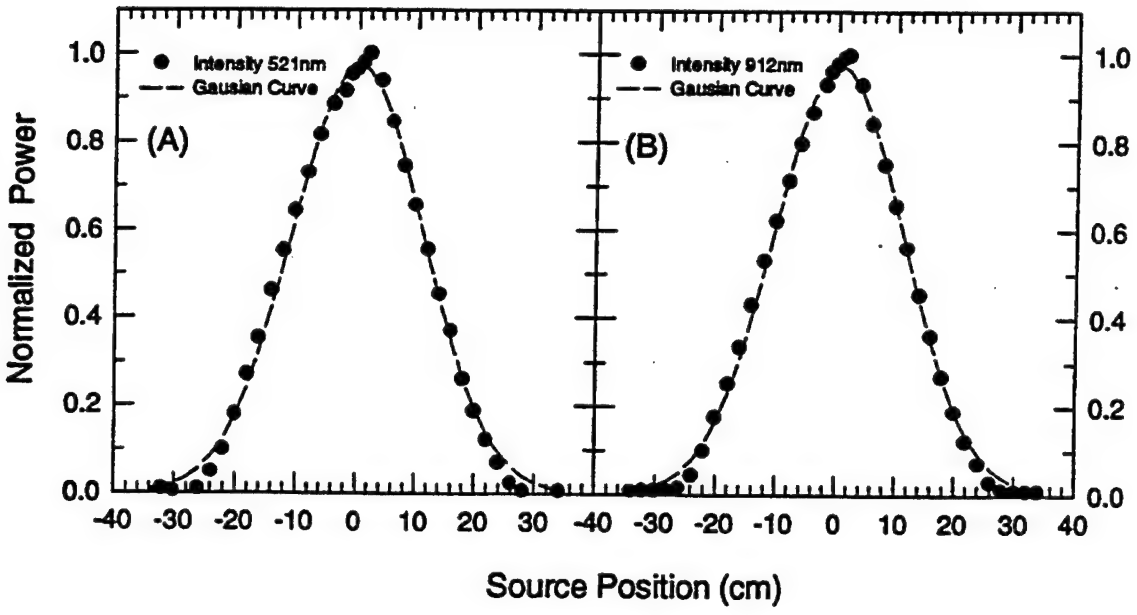

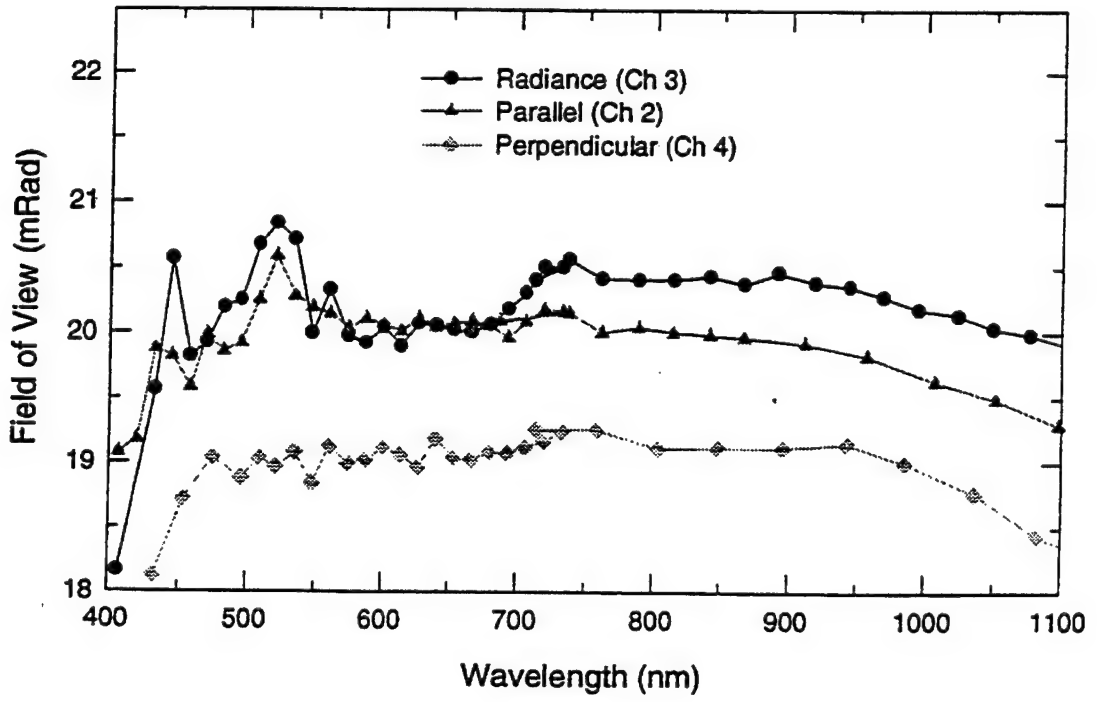

• Figure 5. The characteristics of the field of view of the radiance channels of the SSP1.

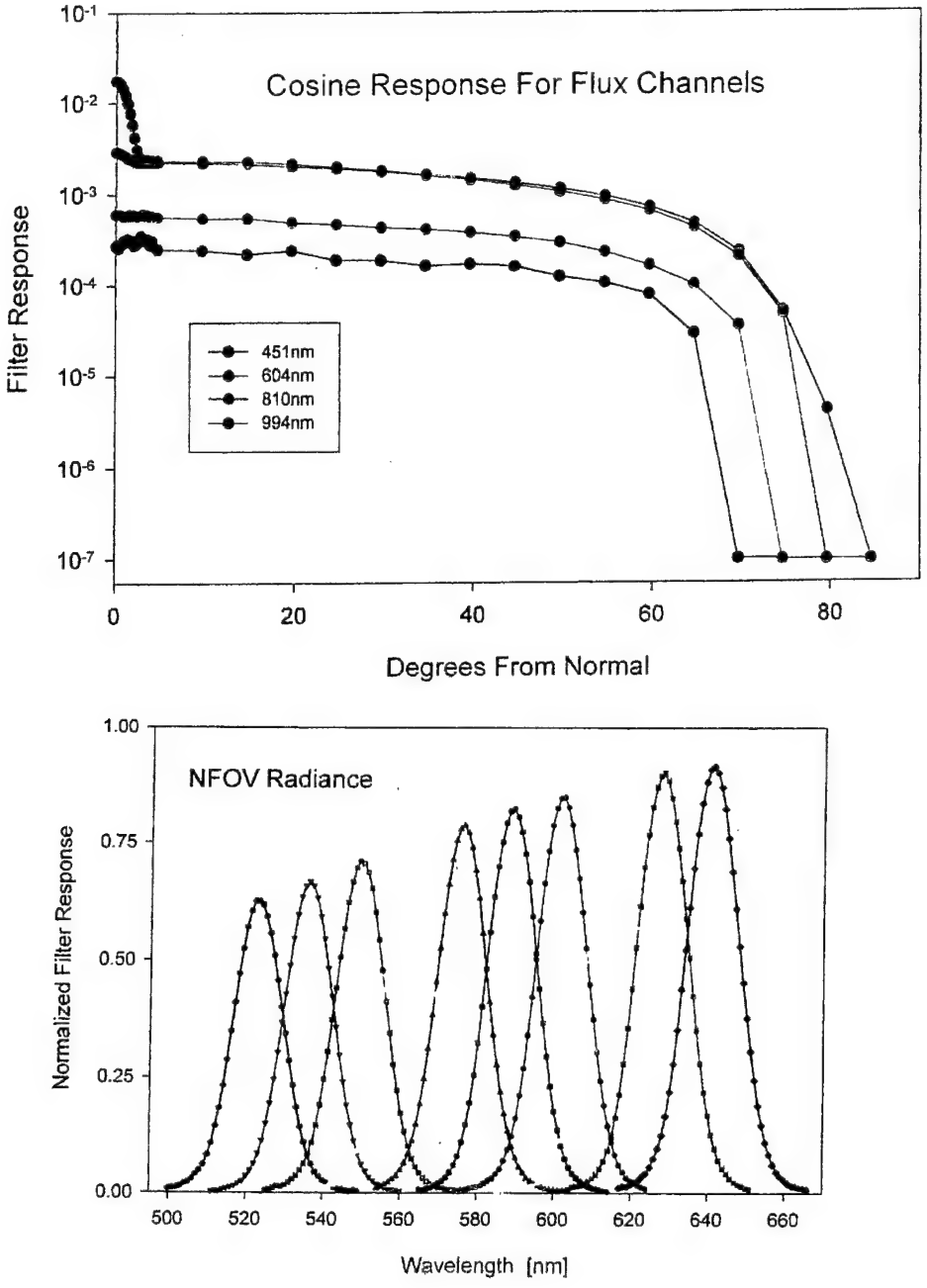

• Figure 6. (top) The cosine response of the diffuser used in the SSP1 and SSP2. (bottom) The spectral bandpass of the CVF for 10 of the channels of the SSP1.

The principal change from SSP1 revolves around the detector and its assembly. The detectors are thermo-electrically cooled (TEC), two color hybrid detectors contained in two miniature packages developed for the SSP2. The two-color detector has a 2mm silicon (Si) photovoltaic detec-

tor mounted over a 1 mm Indium Arsinide (InAs) photovoltaic detector. The Si detector operates from 0.4 μm to 1.1 μm and has a 50% transmission beyond this upper wavelength. The InAs operates in a photovoltaic mode which eliminates the need for bias voltages which are sources of noise that are difficult to eliminate when the instrument is to be operated in a continuous or near continuous mode as proposed. Both detectors operate in a DC mode and are temperature controlled by a two-stage thermoelectric cooler providing superior stable detector performance resulting in a much improved calibration over that of the SSP1. The second package of the detector assembly contains the dual channel hybrid preamps.

The SSP2 electronics consist of a power supply package, a motor drive package, a TEC package, and the main electronics. These four packages have been miniaturized for use on UAVs. The data system is integrated into the main electronics package and contains two microcontroller boards. One is an 8 bit high speed 8051 derivative microcontroller that controls the entire instrument, collects data and sends these data to a 16 kB FIFO. The second computer is a single board miniaturized 486 computer that preprocesses data for output. This preprocessing involves dark current removal, ordering wavelength channels and averaging scans. The SSP is designed to determine the dark current on each scan which can change from scan to scan. The output is approximately 2 Kbytes per scan after preprocessing. A total of 60 A/D channels available with twelve 16 bit channels for optical data, sixteen 12 bit temperature channels, and 32 12 bit channels that monitor the health of the system.

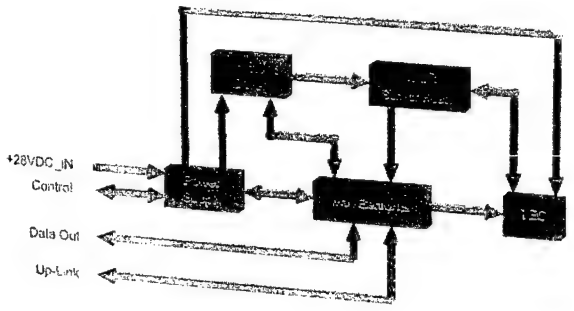

• Figure 7. A block diagram of the main components of the SSP2.

The sensor system (including data system) weighs 10 lb, operates with 28VDC and requires between 4-8 amps to operate depending on the temperature to which the detectors are cooled. Further details of the electrical, mechanical, and optical configurations can be found at the SSP web site at http://optical.atmos.colostate.edu.

Field Applications

The SSP1 radiometer has flown on four different aircraft platforms as part of the ARM-UAV program, the DHC-6 Twin Otter, the GNAT 750 UAV, and the Grob Egrett, and the Altus UAV. It has been regularly flown to

45,000 feet on two different ARM UAV deployments, has been exposed to flight temperatures from -52°C to 20°C, and to calibration temperatures of -65°C.

Examples of Measurements

Figure 8 highlights SSP1 measurements of spectral flux reflected from a thin cirrus clouds observed during the October, 1995, ARM-UAV IOP, and contrasts these against model simulations of the spectrum for similar conditions.

Multispectral Pushbroom Imaging Radiometer (MPIR)

The Multi-spectral Pushbroom Imaging Radiometer (MPIR) developed by Sandia National Laboratories is an imaging radiometer for measuring well-calibrated optical data in nine spectral bands with selected wavelengths ranging from the visible to 11 μm. Figure 9 is a simplified schematic illustration of the MPIR concept, showing how the forward motion of the aircraft is used to convert the radiometric data from linear arrays into a 'pushbroom' image of the object space below. Table 1 shows some image and resolution parameters for both the standard nadir pointing mount

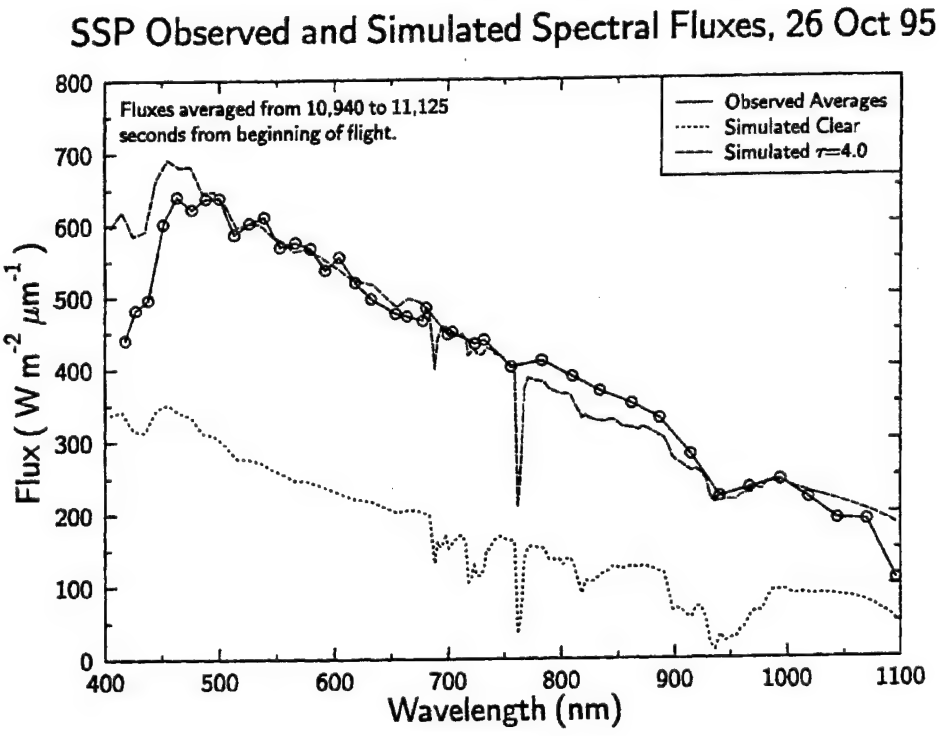

• Figure 8. Reflected spectral fluxes measured above a cirrus cloud during the October 1995 ARESE experiment. The solid curves indicated theoretical prediction.

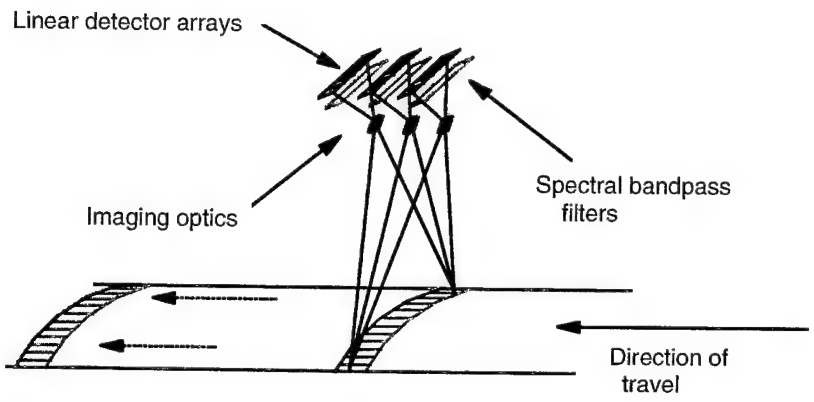

• Figure 9. Basic elements of the Multi-spectral Pushbroom Imaging Radiometer.

and a special 11° port offset mount which increases angular coverage for certain satellite calibrations. Note that the high resolution 0.62-0.67 μm channel has twice the resolution indicated in this table.

MPIR has nine interchangeable detector modules that cover the nine spectral channels. These channels, and their intended usage, are specified in Table 2. Each has its own co-aligned optics, linear detector arrays, signal electronics, and digital signal processors to produce a serial, digital output of the image data. MPIR was designed to operate for extended periods of time from an Unmanned Aerospace Vehicle (UAV) at altitudes from sea level to 20 km. Although selection of alternate spectral bands would make MPIR adaptable to many remote sensing applications, its original nine bands were chosen to provide identification and characterization of cloud properties for use in GCM modeling efforts. Additional information such as surface reflectance, top-of-the-atmosphere radiative fluxes, aerosol concentrations, etc., may also be extracted from the MPIR data.

• Table 1. MPIR pixel widths for various conditions.

Pixel width	*Standard mount*		*Port skewed mount*		
Range	*Port or Starboard*	*Nadir*	*Port*	*Nadir*	*Starboard*
5 km	43 m	29 m	63 m	28 m	33 m
10 km	85 m	57 m	126 m	55 m	65 m
15 km	128 m	86 m	189 m	83 m	98 m
20 km	170 m	114 m	252 m	110 m	130 m

• Table 2. MPIR channel assignments.

Channel	*Bandwidth (μm)*	*Detector*	*Usage*
1	0.62-0.67	Si	A, B, F, G, H, I
2	0.86-0.90	Si	A, F, G, H, I
3	1.36-1.39	InGaAs	C, D, I
4	1.58-1.64	InGaAs	A, B, F, G, I
5	2.11-2.22	InSb	A, B, F
6	3.55-3.93	InSb	A, B, F, I
7	6.54-6.99	HgCdTe	C
8	8.40-8.70	HgCdTe	A, C, D, E, F, H
9	10.3-11.3	HgCdTe	A, C, D, E, F, I

Usage key:
A = cloud identification and amount
B= cloud thickness, particle size, phase
C= upper tropospheric water vapor
D = cirrus detection
E = surface and cloud temperatures
F = surface properties
G = vegetation
H = aerosol detection
I = satellite calibration

To improve radiometric accuracy, an on-board calibration shutter oscillates at 4 Hz in a horizontal plane below the detector modules alternately opening and closing the entrance aperture. A 'main' digital signal processor board controls the shutter movements and synchronizes data taking at a 2- or 4-Hz rate such that each module takes data when the shutter is both open and closed. During the 'closed' data collection the Lambertian black coating on the shutter blades provides a 'dark' reference for the visible channels as well as a blackbody temperature reference for the longer wavelength detectors. The temperature of each shutter blade (measured by a sensor imbedded in each blade) is used in the calibration of each channel as needed. The 'open' data is radiometric data from the scene below. The main processor collects the closed and open data from each module and combines them into an 80kB/sec serial data stream that is telemetered to a ground recording station by the UAV.

Only the modules with InSb and HgCdTe detectors require active cryogenic cooling to 80°K to reduce detector noise below signal levels, how-

ever by design all modules are cooled to stabilize the response of the detectors and collocated electronics for calibration purposes. A separate dedicated microprocessor measures the temperature of each detector focal plane and controls the flow of liquid nitrogen to each module to maintain the desired operating temperature for the detector arrays. Since it is desired to eventually fly multi-day UAV missions, the cryogenic system was designed for minimal cryogen loss and usage rates. The cryogen loss from dewar heat leakage is nominally the same as the module usage rate. The goal was to operate a 48-hour high-altitude mission from the five liter storage dewar pictured in Figure 10. At nominal room temperatures with no module cryogen usage, this five liter dewar must be refilled every 4-5 days.

The basic exposure cycle of the system is 250 ms corresponding to the 4Hz oscillation rate of the near-resonant shutter system. This allows for roughly 80ms of open shutter, 80ms of closed shutter, and 80ms of the shutter being somewhere between open and closed. A conservative exposure time of 60-65 ms is allowed for the open or closed measurements of any module. The analog output from each array element is digitized into 12-bit words in the electronics attached to the module. Several array readouts may be averaged within a 60 ms exposure period to enhance the module signal-to-noise ratio. To approximately match exposure rates to aircraft ground speed, the standard 256-element array modules report data to the main board at a 2 lines/sec rate, while the high-resolution 512-

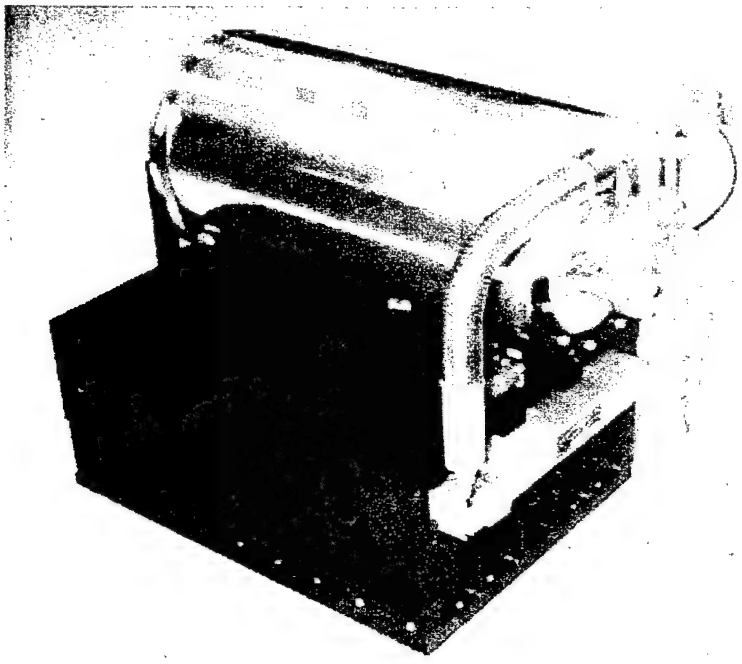

• Figure 10. Exterior view of the MPIR system in a nadir-viewing configuration with its five liter LN_2 storage tank. The optical windows in the bottom surface are not visible.

element modules produce data at 4 lines/sec. All averaged open data is reported to the main processor, but to reduce data transmission rates only closed data statistics averaged over 108 shutter cycles are transmitted. The main processor packs the 12-bit open data, the closed data statistics, system and shutter temperatures, as well as system error words into 4.5kB blocks that are sent in serial fashion to the UAV telemetry system at an 80kB/sec rate. The data is decoded and reassembled into nine separate channel images on the ground.

The four distinct types of detector arrays that are used for MPIR modules are shown in Table 2 above. The maximum number of array elements for each of these are 512 for Si and InGaAs and 256 for InSb and HgCdTe. During the Spring '96 test series flown from the Blackwell/Tonkawa, OK, airport MPIR flew in an Egrett aircraft with the two Si and two InGaAs modules installed and operational. During Fall '96 five modules were aboard for the Altus UAV flights: the 4 from Spring '96 plus one of the InSb modules (2.11-2.22 μm). The hardware for the other InSb and three HgCdTe modules is nearly complete and should be available for future flight series.

Figure 11 shows typical images from the MPIR instrument recorded si-

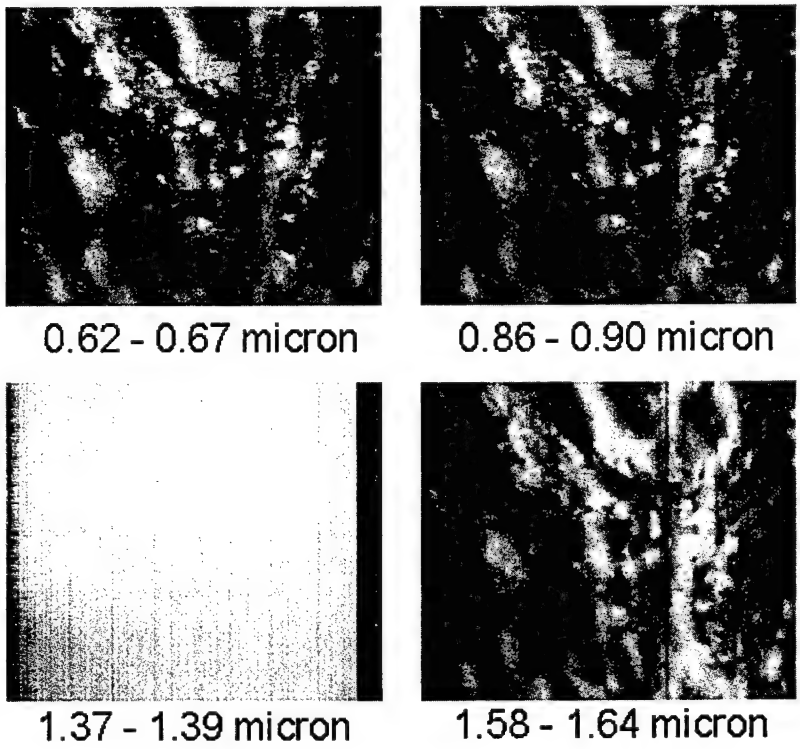

• Figure 11. Four raw-data MPIR images from the Spring '96 test series, 5 May 1996.

multaneously in the spectral bands indicated. The pushbroom data was collected over a 128 second interval centered on 21.4 hours GMT on 5 May 1996. No spatial or shading corrections have been applied to this data which was recorded while the aircraft was in relatively level flight. The striations in the lower two images are artifacts of their linear arrays and will go away once the radiometric calibrations are applied. All data images are displayed here as 256 x 256 element images even though the 0.65 μm channel was recorded at a 512-element resolution. All channels show the same general cloud distribution except for the 1.38 μm which is a water absorption band. This water absorption channel is configured for top of the atmosphere fluxes and at this altitude sees a signal that is only 100-200 counts compared to several thousand for the other bands.

Water Vapor

Two instruments by Brookhaven National Laboratory for measurement of water vapor concentration have been developed for deployment on UAVs under SERDP funding . These development activities were motivated by the constraints of weight, size and power consumption on instruments imposed by the UAV platform, and by the desire of the scientific community to have more accurate and higher resolution water vapor measurements over a range of conditions. Of particular interest to the scientific community was accurate (10%) water vapor measurements at high altitudes (~20 km) where concentrations can be as low as few parts per million.

At the outset of this program, no single instrument was available either commercially or in the research community suitable for measurements of water vapor over the range of conditions envisioned for UAV operations. Available instruments were either too large, weighed too much, or drew too much power for UAV applications. Instruments based upon three different measurement principles were examined. These included: (1) dew point / frost point hygrometers; (2) UV photofragmentation instruments in which water is photofragmented by UV radiation to generate OH radicals, and the water vapor concentration is related to the fluorescence intensity, and; (3) Infrared absorption techniques. It was decided to develop UAV instruments based on two of these measurement principals, dew point frost point hygrometry and infrared absorption. Dew point frost point hygrometry was chosen because it was decided that an instrument based upon this principle was the quickest route to having a useful, although somewhat slow, instrument for high altitude water vapor measurements. The infrared absorption technique were chosen because we feel that instruments based on this technology will be the instruments of choice for high altitude water vapor measurements in the future. These instruments are described below.

Frost Point Hygrometer

This instrument is a modification of a commercial instrument available from Buck Research, Boulder CO. The original instrument comprises a box of electronics of about 17x12x7 inches, a sensing head which is approximately a cube of side 8 inches and a Dewar flask containing 5 liters of liquid nitrogen which give the instrument an operating time of about 15-20 hours. The major problem with this instrument was the size and weight of the liquid nitrogen supply which made it impossible to use on the UAV. In discussions with the manufacturer it was decided that this supply could be replaced by a commercially available Stirling cycle cooler, a cylinder of diameter 1.75 and length 8 inches, which would greatly reduce the volume and weight of the instrument, and allow operation for as long as desired without the need for replacing the liquid nitrogen supply.

A contract was made with Buck Research to modify their standard instrument to operate with a Stirling cycle cooler, and to repackage the instrument to eliminate extraneous weight and volume. The instrument, as delivered weighs less than 10 kg, occupies a volume of only 0.015 m^3, and uses between 90 and 110 W of power, well within the requirements for UAV deployment. Figure 12 shows installation of this instrument in the Altus UAV during the Fall 1996 field campaign.

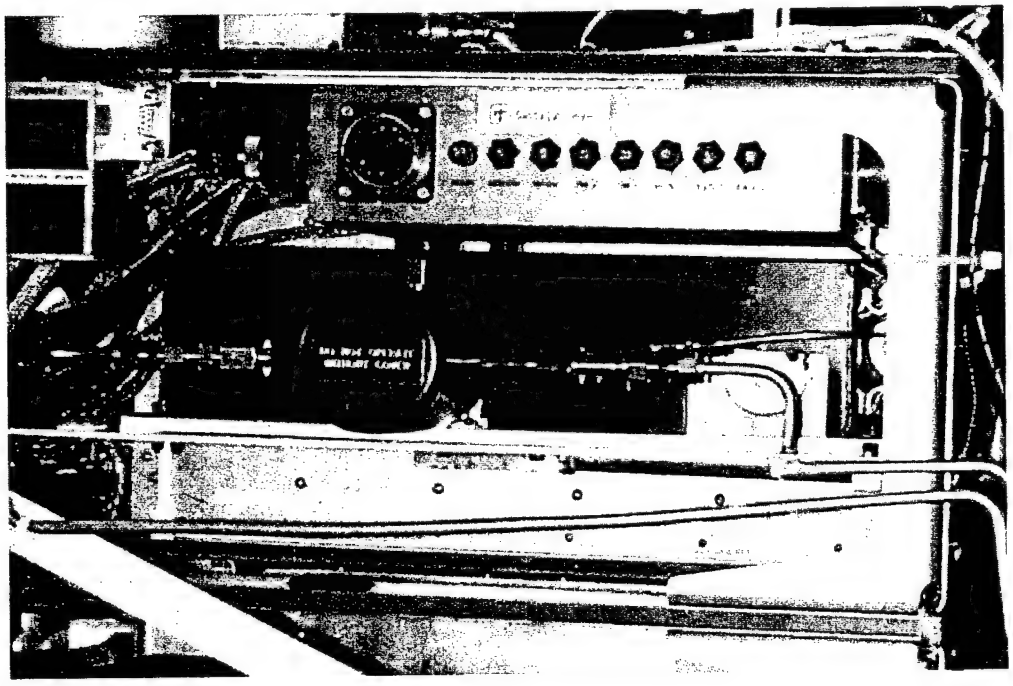

• Figure 12. Frost Point hygrometer as installed in the Altus. Cylindrical component in the center of the picture contains the sensor. Box to which sensor is attached contains the electrons and the Stirling cycle cooler.

The instrument was delivered in the Fall of 1995, and after rigorous testing and calibration in the laboratory (including altitude chamber tests), was deployed during the Spring 1996 UAV experiment. The principal problem encountered during the initial deployment was providing sufficient cooling to the sink side of the Stirling cooler to allow for extended operation of the instrument at high altitudes. For the initial deployment this was accomplished by adding a cooling fan to the instrument. For subsequent deployments we have connected the waste heat side of the cooler to a heat pipe which conducts the heat to the outside airstream. We feel that such an arrangement will allow use of the instrument to altitudes of about 15 km. This mode of operation was successfully demonstrated during the Altus UAV flights in September 1996.

The instrument operated well during both deployments in 1996. Dew points as low as -80° C were measured at altitudes up to 13 km. These dew point measurements compared favorably with measurements made by radiosondes released during the flights and to a conventional thermoelectrically cooled hygrometer during intercomparison flights.

Tunable Diode Laser Hygrometer

An instrument has also been developed based upon infrared absorption using a tunable diode laser (TDL) as a source. Although infrared absorption instruments utilizing TDL sources have been under development for some time, construction of a lightweight compact instrument suitable for UAV deployment has only recently been made possible by the development of a InGaAsP diode laser. This TDL operating at 1393 nm where water vapor strongly absorbs is lightweight, uses little power, and does not require large cooling systems to maintain its stability. Previous to the last few years, TDL instruments were based upon on lead salt diode lasers, operating in the chemical infrared. These have several disadvantages which include the need to cool both the lasers and detectors to cryogenic temperatures and difficulty in reproducibly matching frequency with a particular absorption line. The near infrared lasers are far easier to use and require less ancillary equipment, which in turn reduces the power draw and the weight, and makes an instrument for UAVs possible.

TDL sources have the immense advantage over other infrared sources in that they can be quickly (10 kHz-1 MHz) scanned across the narrow (3 GHz) absorption, thereby removing drift and most of the other noise. Presumably, the most significant source of inaccuracy would be drift and non-linearity in the amplifiers and other electronic components. Since a good deal is known about stabilizing electronics this should not be a major problem. Theoretically, slow changes in the laser power, the reflectivity of the retroreflector, transmission of the windows, etc. should have no effect on the calibration.

To take advantage of this emerging technology, a contract for development of a UAV compatible instrument was let to Southwest Sciences Inc., Santa Fe, NM in the Fall of 1995. A prototype instrument has just been completed, began testing in the fall of 1996, and will be ready for the next UAV deployment in the Fall of 1997. The instrument is configured in a way that allows the measurement of water vapor external to the aircraft. A sensor head containing the source and detector will protrude from the aircraft; a retroreflector will be mounted approximately 2 m away on the aircraft fuselage or wing to form the measurement path. In comparison to an internal cell, this configuration minimizes payload volume, and minimizes time response problems associated with adsorption of water vapor on instrument surfaces. The instrument meets the specifications listed in the Table 3. Actual characteristics await further tests in the laboratory and accumulation of some flight experience.

• Table 3. List of TDL instrument specifications.

Specification	*Value*
Weight	<20 kg
Power	75 W, 28 VDC
Volume	0.03 m^3
Absolute [H_2O] accuracy	10%
Minimum Frost Point	-88° C
Response Time	1 sec
Maximum altitude	20 km
Interior Temperature	0-30° C
Interior Pressure	same as exterior
Period of unattended operation	60 hrs

Radiative Instruments

The accurate measurement of radiances and radiative fluxes in the atmosphere is key to improved understanding of atmospheric physics, including effects of greenhouse gases and clouds on the Earth's radiation budget. For example, General Circulation Models (GCMs) indicate that a doubling of atmospheric CO_2 will change the net flux at the top of the atmosphere by 3-4 Wm^{-2}, with concomitant changes in surface temperatures of 1.5°-4.5°C.[1] The prediction of this kind of temperature rise of course requires the accurate modeling of many diverse physical phenomena, among them the interaction of solar radiation and clouds. However, Pilewskie, Valero,[2] and many others have been recently reviewing experimental evidence that suggests that cloudy atmospheres absorb sev-

eral tens of watts per square meter more than portrayed in GCMs. If this additional absorption is verified, then the GCMs need to be corrected to improve the accuracy of their greenhouse warming predictions.

To further the state of the art in making radiation cloud measurements, the ARM-UAV program has undertaken the development of two radiative instruments for highly accurate measurement of shortwave and longwave radiation in the atmosphere from UAVs.

The Hemispheric Optimized NEt Radiometer (HONER) measures shortwave and longwave hemispherical broadband fluxes using differential radiometry, chopping the signal from upwelling and downwelling fluxes onto a single AC detector system. This permits true optical differencing for unprecedented accuracy in measuring net fluxes

The AERI-UAV makes high spectral resolution (0.3-0.5 cm^{-1}) observations of atmospheric emission from 3-25 μm, providing important meteorological information related to atmospheric state parameters (temperature, water vapor, and other greenhouse gases), cloud and surface spectral properties, and processes influencing radiative budgets and regional climate.

Hemispherical Optimized Net-flux Radiometer (HONER)

Introduction

Making highly accurate flux, and especially net flux, measurements is difficult. Net flux is usually derived by differencing up welling and down welling hemispherical fluxes. Commonly, pyranometers and pyrgeometers are used to measure these hemispherical fluxes on ground based platforms. These instruments have typical calibration spreads of ±7% according to results at National Renewable Energy Laboratory (NREL)[3], with best results at ±3.5%, and a drift of order one percent per day. To obtain a net flux, one generally takes the mathematical difference between the measured upwelling and downwelling fluxes, leading to large errors (typically tens of Wm^{-2}) in the net flux. In the area of airborne instrumentation, some very good results have been obtained using other types of radiometers for individual upwelling and downwelling fluxes.[4,5] Net fluxes have also been derived from radiance measurements, which are converted to fluxes using models, and from measurements made in spectral bands, which must also be converted to fluxes using models. Temporal and spatial sampling strategies add further errors, which may be unavoidable in realistic experimental scenarios.

The net radiation in a volume is deterministic for the local heating or cooling of the atmosphere and is obtained by some combination of airborne and ground based measurements. Since some individual processes can

have quite large local effects, progress can, and has, been made with measurements of the available accuracy.[6] The present state of measurements, however, requires improvement to achieve the next steps in understanding radiative transport.

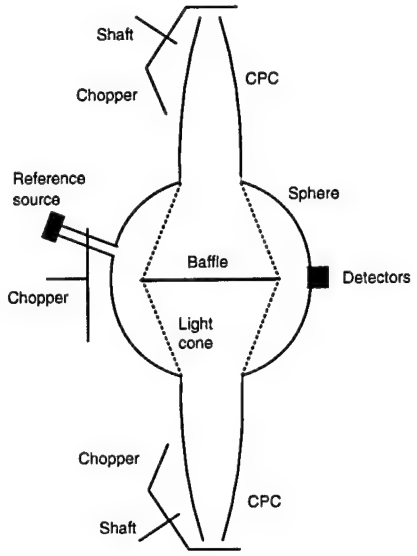

• Figure 13. Schematic of One HONER Integrating Sphere.

The Hemispheric Optimized NEt Radiometer (HONER) has been developed by Los Alamos National Laboratory (LANL) to improve measurement accuracy in several ways. (1) HONER uses differential radiometry, chopping the signal from upwelling and downwelling fluxes onto a single AC detector system, allowing true optical differencing for unprecedented accuracy. (2) HONER also measures the individual fluxes, with the ability to reconfigure from differential to direct mode in flight. (3) HONER calibrations are performed using NIST standards, and the calibration is maintained continuously during operation using on-board reference sources. (4) Wavelength coverage is from UV to 1.2 μm, 1.2 - 4.5 μm, and 4.5 to >50 μm. (5) Information is provided separately in shortwave and long wave bands to facilitate comparisons to models. Additional information can be added in selected wavelength intervals as appropriate to elucidate further physics.

Configuration

HONER comprises two integrating spheres, one of which is shown schematically in Figure 13. Each sphere has two input apertures; one looking downward and the other upward. Radiation entering the input apertures is propagated into the sphere by means of an inverted compound parabolic concentrator (CPC).[7] The geometry of the input apertures is such that the instrument has a 170° field-of-view; the remainder of a 180° field-of-view being obscured by structure surrounding the aperture. The radiation through each aperture is chopped at the same frequency, 19.2 Hz, but out of phase. The phase relationship determines the operating mode and will be discussed later.

Wavelength Response

One sphere is lined with Spectralon, Labsphere Inc.'s trade name for a diffuse reflecting material, and the other is coated with a Lambertian gold, also proprietary to Labsphere. The Spectralon provides sensibly flat reflectance from the UV to nearly 2 μm and the gold provides flat reflectance at all wavelengths longer than the visible region.

Each sphere also contains two channels of pyroelectric detectors and each channel uses distinct filters. To aid in achieving insensitivity to the direction of arrival of the incident radiation, each channel comprises four detectors distributed at 90° intervals about the sphere's equator. In the interests of spectral uniformity, reproducibility, stability, and low cost, the filters consist of uncoated silicon and water free fused silica. Thus, the filters define spectral bands of each channel, designated SW1, SW2, LW1, and LW2 as summarized in Table 4. The spectral responses of these channels are shown in Figure 14 and Figure 15.

Channel SW1 provides uniform response to radiation in the wavelength from the UV to the silicon band gap at 1.2 μm. There is also a response to radiation from 1.2 μm to the silica cut-off at approximately 4 μm but, due to the spectrally non-uniform response generated by the Spectralon reflectivity, this is not directly usable in measuring the flux in this spectral region. Channel SW2 responds only to the 1.2 to 4 μm band in a manner which, within a constant factor, is identical to the response of SW1. Therefore, by subtracting the properly scaled output of SW2 from the output of SW1, we have a good measure of the total irradiance at wavelengths shorter than 1.2 μm.

Channel LW1 provides a good measure of the total irradiance at all wavelengths longer than 1.2 μm and channel LW2 provides a good measure of the irradiance between 1.2 and 4 μm. Adding the information gained from LW2 as a relatively small correction to that obtained from the short wave sphere provides a measure of the irradiance in the solar dominated portion of the spectrum, from the UV to 4 μm. Subtracting

• Table 4. HONER Channel Responses.

Channel	*Sphere*	*Filters*	*Band*
SW1	Short Wave	SiO2	UV to 4.5 μm
SW2	Short Wave	SiO2+Si	1.2 to 4.5 μm
LW1	Long Wave	Si	1.2 to >50 μm
LW2	Long Wave	SiO2+Si	1.2 to 4.5 μm

LW2 from LW1 provides a measure of the irradiance in the thermal IR, 4 μm and longer.

Reference Sources

The HONER integrating spheres serve as comparators between the unknown fluxes incident on the CPC apertures and reference fluxes generated by calibrated sources and delivered to the sphere by optical conduits and modulated by a third mechanical chopper. HONER uses both a short wave reference ($\lambda < 1.2$ μm) and a long wave one ($\lambda > 1.2$ μm).

The short wave reference source is a 2.5 watt, quartz halogen lamp rated at 36 lumens output. To accommodate the short mean lifetime of these lamps four, one operating and three spares, are mounted in a 5 cm diameter integrating sphere; that arrangement also negates the geometric effects of lamp position. The output of this lamp is modulated by a third chopper blade at 28.8 Hz (exactly 1.5 times the main chopper frequency) and delivered to the main integrating sphere of each sensor system. The output of the lamp is monitored with two differently filtered silicon photodiodes in the main integrating sphere. Using the outputs of these photodiodes, the filament power and thus output of the lamp is controlled to a constant color temperature; subsequently the output of either of the photodiodes is used as an indicator of the total flux delivered by the color temperature stabilized reference source. This source provides us with a known radiance by which we determine the slope of the responsivity curve, since the intercept is known to be zero because the admitted flux is zero when the aperture is closed.

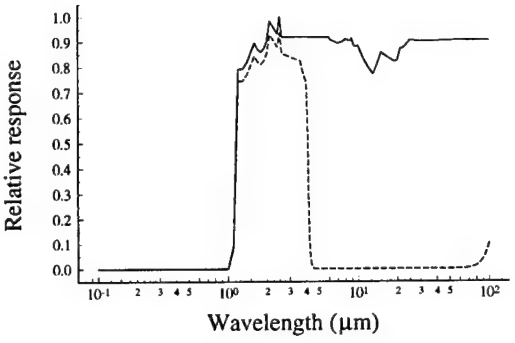

• Figure 14. HONER Longwave Response.

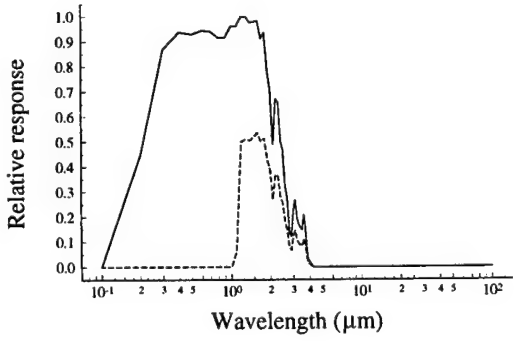

• Figure 15. HONER Shortwave Response.

The long wave reference is a small, dark body (uniformly high emissivity but not necessarily black) emitter. As with the short wave reference, this source's emitted radiation is modulated at 28.8 Hz. The chopper blade is also a dark body emitter, operating at a temperature similar to that of the integrating sphere and is monitored to within 0.1K. The temperature of the reference source is held at either 330K or 30K above the blade temperature, whichever is less. Thus, the long wave reference radiation is modulated between two known levels, permitting determination of the slope and intercept of the signal vs. flux function.

When HONER is operating in the absolute mode, the intercept of the long wave responsivity curve is the self-emission of the integrating sphere which is reflected back into the sphere when the entrance aperture is closed by the main chopper. In the differential mode, this quantity cancels from the analysis and the intercept is zero. It does, however, form the basis of the requirement that the temperature of the long wave integrating sphere be known with high accuracy. We constructed the sphere with a quarter inch thick aluminum wall to reduce thermal gradients and measure the temperature using several thermistors. By this means, we expect to know the radiation temperature within 0.1K.

Air Flow Control

The ideal situation relative to radiation transfer is for HONER to be flown with open apertures. However, this leaves the instrument at risk to thermal perturbations caused by net air flows through the spheres. A window at the internal aperture, the junction of the CPC and the integrating sphere, represents a compromise between the risk of air flows and several adverse optical effects. For example, the maximum angle of incidence on a window at the internal aperture is 17.5°, thus reducing the sensitivity to angle of incidence and polarization. The short wave sphere requires a silica filter (window) for both channels at the internal aperture, and also in the path of the radiation from the short wave reference source. Similarly, as the long wave sphere requires a silicon filter (window) for both channels at the internal aperture and in the paths of the radiation from the long wave reference source. Thus, the integrating spheres and detectors are well isolated from air flow effects, assisting in the temperature control effort.

The silicon windows produced for use at the internal aperture required some attention and innovation. We require them to be relatively thin to minimize the effect of the 9 and 17 μm absorption bands but they must withstand the vibrations associated with aircraft deployment despite having a diameter greater than 80 mm. Rockwell International in Albuquerque ultrasonically machined a silicon cruciform in a ring of the window diameter and bonded it to a 0.5 mm thick window using a glass frit. This assembly is quite capable of withstanding the mechanical environment

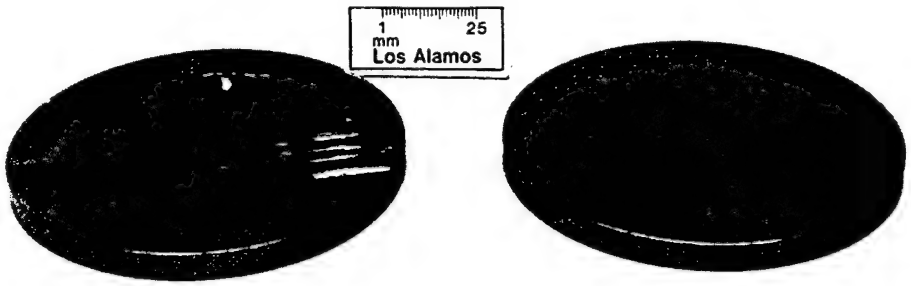

• Figure 16. HONER Silicon Window Assembly.

while providing the transmittance of a thin silicon window with only a modest loss due to the cruciform. This window is shown if Figure 16.

A fairing around each aperture was designed to minimize air entrainment through the aperture. To verify the design, a half-size model was constructed and tested in a wind tunnel at New Mexico State University in Las Cruces. The results of this test indicate that in all but the most extreme maneuvers, air entrainment through the apertures is minimal. In addition, a small amount of air, entering a duct at the nose of the fairing, is heated with waste engine heat and introduced to the base of each CPC near the internal aperture window. The small pressure and flow thus generated was to assist in keeping unconditioned air out of the instrument, stabilize instrument temperature, and prevent internal moisture condensation. Mechanically actuated "eyelids" at each aperture were designed to seal HONER from contamination such as dust generated during take-off and landing or rain.

Signal Multiplexing

The main aperture choppers, with two apertures on each blade, operate at 19.2 Hz but either 90 or 180° out of phase. When these choppers are 90° out of phase, HONER is operating in the absolute mode making independent measurements of the upwelling and downwelling irradiances. When these choppers are 180°out of phase, HONER is operating in the differential mode measuring the difference between these irradiances. The third chopper, modulating the reference flux, operates at a frequency precisely 1.5 times that of the main choppers. This is achieved by operating the reference blade, having three apertures, in mechanical synchronization with the other two.

When the choppers at the two input apertures are 180° out of phase, the flux on the detectors is a square wave whose amplitude is proportional to

the difference between the irradiances on the upward-looking and downward-looking apertures. When these choppers are 90° out of phase, the detector output, in response to the upwelling and downwelling irradiances, is the superposition of two periodic functions whose fundamentals are proportional to the sine and cosine, respectively, of 19.2 Hz. The detector response to the reference flux on either sphere is a periodic function whose fundamental is at 28.8 Hz.

The relative mechanical phase of the choppers is controlled to one part in 1024 of a revolution. The stability of the phase lock is more than one order of magnitude better. Recalling that there are two cycles of the optical phase per revolution of the main choppers, we have that the relative phase of the optical signals is stable to better than 0.1°.

Deployment

An obvious necessity for any aircraft borne instrument having two near-hemispherical fields-of-view is that the aperture separation must be sufficient to exclude the aircraft from the fields-of-view. HONER was designed to be carried by a Perseus B, unmanned aircraft which is produced by Aurora Flight Sciences Corp. One sensor head will be carried in the nose of each under-wing fuel pod. With an aperture separation of 61 centimeters, the aircraft obscures only 1.7% of both, 170° fields-of-view.

Data Acquisition

Data from the signal channels on each sphere are strobed onto 12 bit A/D converters synchronously with the clock used to control the chopper phase. Thus, the phase angle for each datum will be known precisely and the phase interval will be uniform. The two spheres operate asynchronously. We acquire 256 data from each channel over 16 revolutions of the 19.2 Hz chopper, approximately 1.6 second. The housekeeping data, which include the temperatures, reference source status, and chopper phase information, are acquired asynchronously.

Calibration

The results obtained from a precision radiometer are necessarily limited by the accuracy of the calibrations. HONER is calibrated at Los Alamos. LANL possesses and uses calibrated sources and reference detectors which cover the spectral region from the ultraviolet through the thermal infrared. Each of the devices which we use as the basis for the HONER calibration has a 3σ accuracy of 1% or better, traceable to NIST standards. The issues which are addressed in the calibration procedures are absolute response to collimated and diffuse irradiances, sensitivity to variations in direction of arrival, equivalence of the two entrance apertures, sensitivity to variations in wavelength, and sensitivity to polarization.

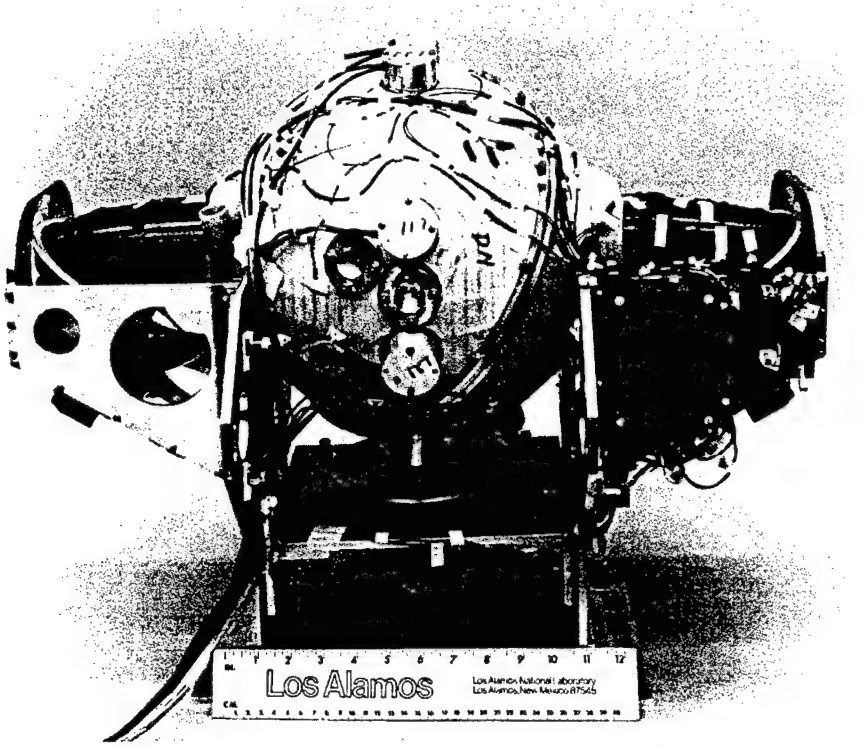

• Figure 17. HONER Assemblage Without Thermal Protection.

Summary

HONER is complete and in the laboratory awaiting final calibration. The long wave sphere, prior to the application of the thermal insulation, is shown in Figure 17. This view shows all essential components of the sensor. By implementing the concept of differential optical radiometry while maintaining the capability for absolute radiometry in HONER, we have designed an instrument capable of providing improved measurements of atmospheric heating due to radiative flux.

UAV Atmospheric Emitted Radiance Interferometer (UAV-AERI)

Background and Scientific Rationale

The Atmospheric Emitted Radiance Interferometer for an Unmanned Aerospace Vehicle (AERI-UAV) was developed by the University of Wisconsin to make high spectral resolution (0.3-0.5 cm^{-1}) observations of atmospheric emission over the spectral range of 3-25 μm, thus providing key meteorological information related to atmospheric state parameters (temperature, water vapor, and other greenhouse gases), cloud and surface spectral properties, and processes influencing radiative budgets and

regional climate. The AERI-UAV uses state-of-the-art Fourier Transform Spectroscopy (FTS), or Michelson interferometry, which has proven to be an exceptionally effective approach for making these IR spectral observations with the high radiometric accuracy necessary for weather and climate applications. Two major advantages of a FTS design that have been recognized for several important applications are (1) the small instrument size, and (2) the high spectral integrity inherent in the FTS laser

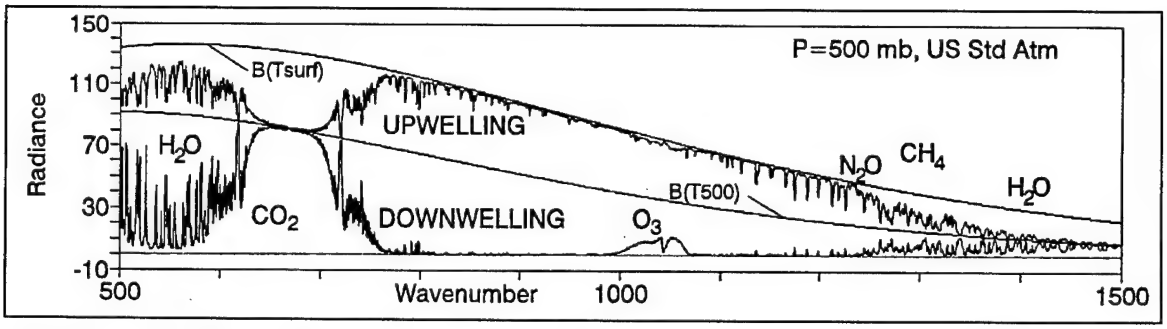

• Figure 18. Simulation of partial AERI-UAV spectra from 7 to 20 microns.

reference approach.

Some of the important new capabilities of the AERI-UAV stem from its capability to observe both upwelling and downwelling radiance. The general nature of these observations is illustrated in Figure 18 by calculated upwelling and downwelling spectra at the 500 mb level in the US Standard Atmosphere for the 7-20 μm region (full coverage includes 3.3-25 μm). The higher radiance upwelling spectrum is bounded by the Planck radiances for the surface temperature and the 500 mb temperature and the downwelling spectrum by the Planck radiance for the 500 mb temperature and zero. The variable opacity of the greenhouse gases is apparent from the structure of the individual absorption lines, with the radiance of the more opaque regions being determined by the local atmospheric temperatures. With this temperature information, the difference of spectra observed from two nearby altitudes gives accurate measures of the absorption (or transmission) of the intervening layer.

A summary of some key science applications of the AERI-UAV is given in Table 5, along with a list of the specific products which can be derived from the fundamental calibrated radiance product. In addition to providing a wide range of spectral radiance and remote sensing information, the AERI-UAV will give spectral cooling rates and effectively in situ cloud and state parameter information from upwelling and downwelling radiances acquired by flying constant-altitude steps.

Table 5. AERI-UAV Science Applications and Data Products.

• Science Applications	• Products
1. More Sensitive Testing of Atmospheric Spectroscopy	1. State Parameters from Remote Sensing
2. Improve Parameterizations of Cloud Microphysics and Radiative Transfer	2. More Accurate Water Vapor and Stability*
3. Observe Greenhouse Contribution from the Radiatively Active Trace Gases	3. Radiative Cooling Rates*
4. Study the Spectral Radiative Forcing of Dynamical Processes	4. Cloud Extinction and Optical Depth Spectra*
	5. Profiles of Cloud Microphysical Properties*
	6. Absorption Coefficent Profiles*
	7. Trace Gas Mixing Ratio Profiles*
	8. Surface Spectral Emissivity

*Accuracy Enhanced from in situ measurements of vertical divergence

AERI-UAV Instrument Design

The AERI-UAV is a third generation instrument, building on successes with a much larger airborne High Performance Interferometric Sounder (HIS) and ground based AERI. Its fundamental design was driven by the need to minimize size, weight and power because of the limited payload capacities of unmanned aircraft. In addition to substantially reducing the size compared to HIS and AERI, the requirements for the AERI-UAV include maintaining high radiometric and spectral calibration accuracy, while providing a instrument that is easy to operate and maintain. These latter factors led to a design that includes the fundamental FTS approach with accurate laser controlled sampling and includes a mechanical detector cooler to eliminate the need for liquid cryogen. The novel aspect of the design, a "4-color" shared focal plane detector configuration described in more detail below, followed from the size and power constraints; this configuration eliminates the need for dichroic beamsplitting and multiple coolers.

The general characteristics of the AERI-UAV are provided in Table 6 and the layout of the instrument is shown in Figure 19. The 45° scene mirror rotates to select views of the atmosphere or of calibration reference sources (one near ambient temperature and one at a stabilized temperature up to 60° C). A typical operational plan when flying at fixed altitudes in the troposphere is to alternate nadir and zenith viewing, with calibration cycles interspersed periodically.

The data is compressed onboard to reduce the data volume requirements for the real-time down link from the UAV. Four forward and four reverse scans are co-added and each are compressed separately. An efficient complex numerical filtering technique is applied using a TMS320C40 Digital Signal Processor (DSP). This information preserving convolution

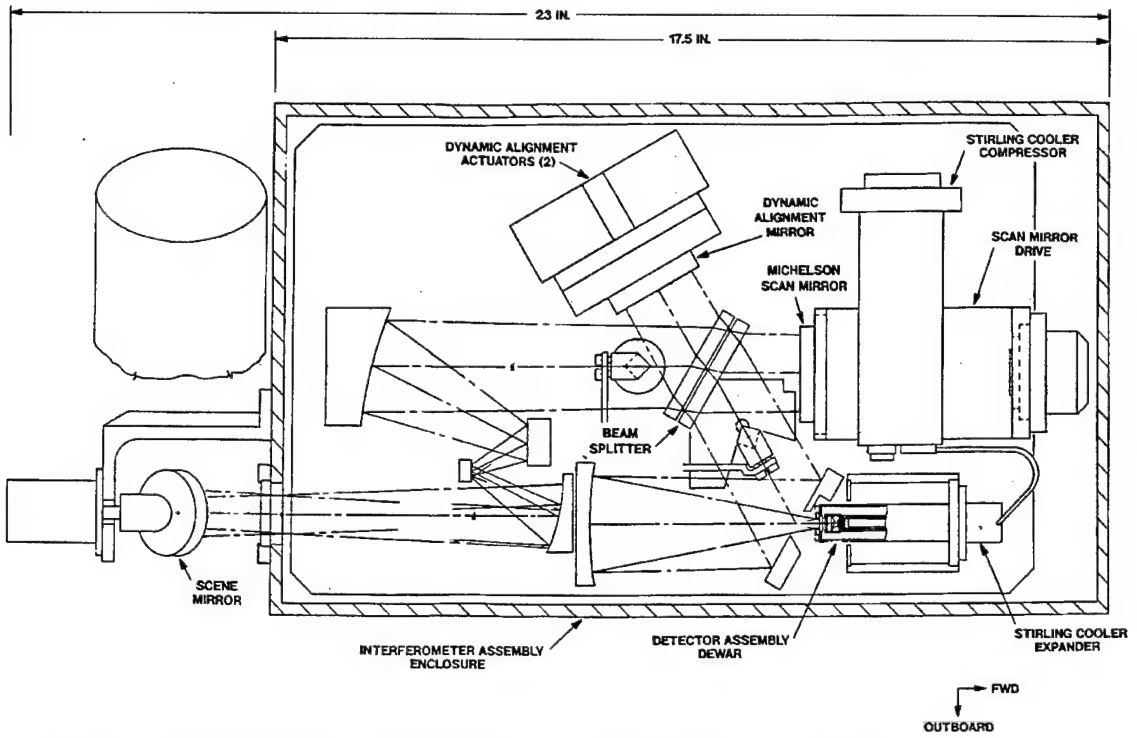

• Figure 19. AERI-UAV top view assembly diagram, illustrating IR beam optical design with laser pick-off mirrors.

filter is followed by bit trimming for delays not close to the zero path difference. A second DSP is used for instrument control.

Radiometric Performance

The radiometric noise and calibration performance of the AERI-UAV is driven to a high standard both by requirements for temperature and water vapor remote sensing and for spectroscopic applications. The RMS noise level in terms of brightness temperature achieved for HIS and AERI is generally less than about 0.2 K, except near the edges of spectral bands and in some localized spectral regions. The performance of the AERI-UAV is expected to be comparable for its 4 second dwell time, except for the extra longwave (ELW) band where longer averaging times will be needed.

The AERI-UAV will make use of the calibration techniques developed for the HIS and also demonstrated by the AERI. The calibration requirements are often stated as: <1 K absolute uncertainty at a brightness temperature of 260 K and reproducibilities (excluding noise) of <0.2 K. The calibration blackbodies used by the AERI-UAV are scaled down versions (62% smaller due to smaller beam diameter at blackbody aperture) of those used by the AERI. These blackbodies are very well characterized and have proven to be very stable over time. Calibration techniques have

been developed that use primary temperature and electrical resistance standards traceable to the National Institute for Standards and Technology (NIST), and a reflectance transfer standard traceable to the National Physical Laboratory. Blackbodies calibrated using these techniques have absolute temperature errors of less than 0.04 K peak-to-peak and an absolute emissivity error of less than 0.001, which translates to a temperature error of 0.10 K peak-to-peak in the longwave band.

• Table 6. AERI-UAV instrument specifications.

Spatial Resolution	100 mrad Nadir, Zenith, & intermediate angles
Spectral Resolution	0.5 cm^{-1}
Interferometer Type	Voice Coil Dynamically Aligned Plane Mirror (Custom Bomem DA-5)
Optical Path Drive/	Flex Pivot Porch Swing; ±1.037 cm; 4 cm/s
OPD Sampling Reference	HeNe Laser with; white light at startup
Fringe Counting	1/4-wave quadrature, continuous back/forth
Interferometer Beam diameter	4.5 cm
Interferometer Angular FOV (full)	40 mrad
Spectral Bands	Extra LW: 19-25 μm LW: 10-19 μm MW: 5.5-10 μm SW: 3.3-5.5 μm
Detectors	InSb over 3-Segment MCT Array
Cooler / Temperature	0.6 W Stirling Cooler (Litton); 68 K
Dwell Time / # Interferograms	4 sec; 4 fore/4 back
Onboard Processing	DSP Numerical Filters
Raw Data Rate	80 Kbps
Mass / Size	45 Kg; 0.05 m^3
Power	160 W

Calibration Facilities

Introduction

The original ARM Program Plan lists the required observations, with accuracies, precisions, temporal resolution, temporal reporting interval, spatial resolution, spatial distribution, spectral resolution and spectral range. The ARM emphasis on needed accuracies continues to the present: the Science Plan of 1996 states: 'ARM should strive to have its radiation flux data be at least ten times as accurate as any other field program, and should not be satisfied with past low standards of performance."

The experiment design issue for the evolving ARM UAV SERDP program was addressed in Spring 1992, and reflected this ARM emphasis on measurement accuracy. As a specific example, linear sensitivities were provided for broad band radiative fluxes as a function of temperature, humidity, cloud fraction, cloud height, atmospheric constituents and aerosols: this pointed to necessary accuracies in the measurements. At about the same time, the JASON review of the CHAMMP Program noted that the atmospheric problem is likely to be nonlinear with near-cancellation of large effects in, for example, cloud physics, Potential measurement requirements were identified, with challenging accuracy goals.

The SERDP / ARM-UAV Program management decided that all calibrations should be referenced to the same NIST-traceable standards, and targeted challenging accuracies for the radiometric calibrations. Appropriate equipment and infrastructure were established at Los Alamos for this task, and are described in the following paragraphs.

Radiometric Calibration Laboratory

The Los Alamos radiometric calibration laboratory is a 4000 sq. ft. facility equipped with state-of-the-art NIST-traceable optical and infrared radiation sources and radiometers, along with IR-Visible-UV spectrometers, and HeNe, GreenNe and CO2 lasers. It can provide for the complete calibrations of instruments in the spectral range 0.5 through 12 μm in both the radiometric and spectral domains; broad-band calibrations extend well beyond this range.

Calibration sources for the thermal IR, for use under ambient conditions, include: (1) a NIST-designed and calibrated fluid bath conical cavity blackbody with a 4 inch diameter aperture, with operating temperature between 280 to 353 K -- the mate to an identical transfer standard blackbody source at NIST. The fluid bath maintains temperature uniformity and stability of 1 mK., and cavity interior temperature uniformity of better than 20 mK.; (2) A gold freezing point (1337 K) primary standard blackbody; (3) A high temperature spherical cavity blackbody (temperature to

3000 K); (4) a commercial (Mikron) spherical cavity blackbody (temperature to 500 K); (5) a commercial (Graseby) conical cavity blackbody (temperature to 1300 K); (6) a CI flat plate black body (temperature to 373 K). Broad band sources for the near IR-visible-UV include: (1) Two commercial Labsphere integrating sphere extended sources with spectral radiance calibrations at the 2% (3σ) level over the 0.3-2.4 μm range, (2) NIST ribbon filament radiance standard lamps, (3) NIST FEL irradiance standard lamps. A low-temperature fluid bath blackbody capable of temperatures down to 200 K is also being fabricated. LANL sources are summarized in Figure 20.

Calibrated detectors include (1) a Cambridge Research cryogenic cavity electrical substitution radiometer with absolute accuracy of 0.02% - 0.05% (1σ) and spectrally flat response from 0.25 to 40 μm. (2) Two Eppley AHF absolute cavity electrical substitution radiometers, designed to measure direct normal-incidence solar radiation at the 0.1% (1σ) accuracy level. These two instruments were recently tied to the World Radiometric Reference through their participation in an ARM-sponsored intercomparison

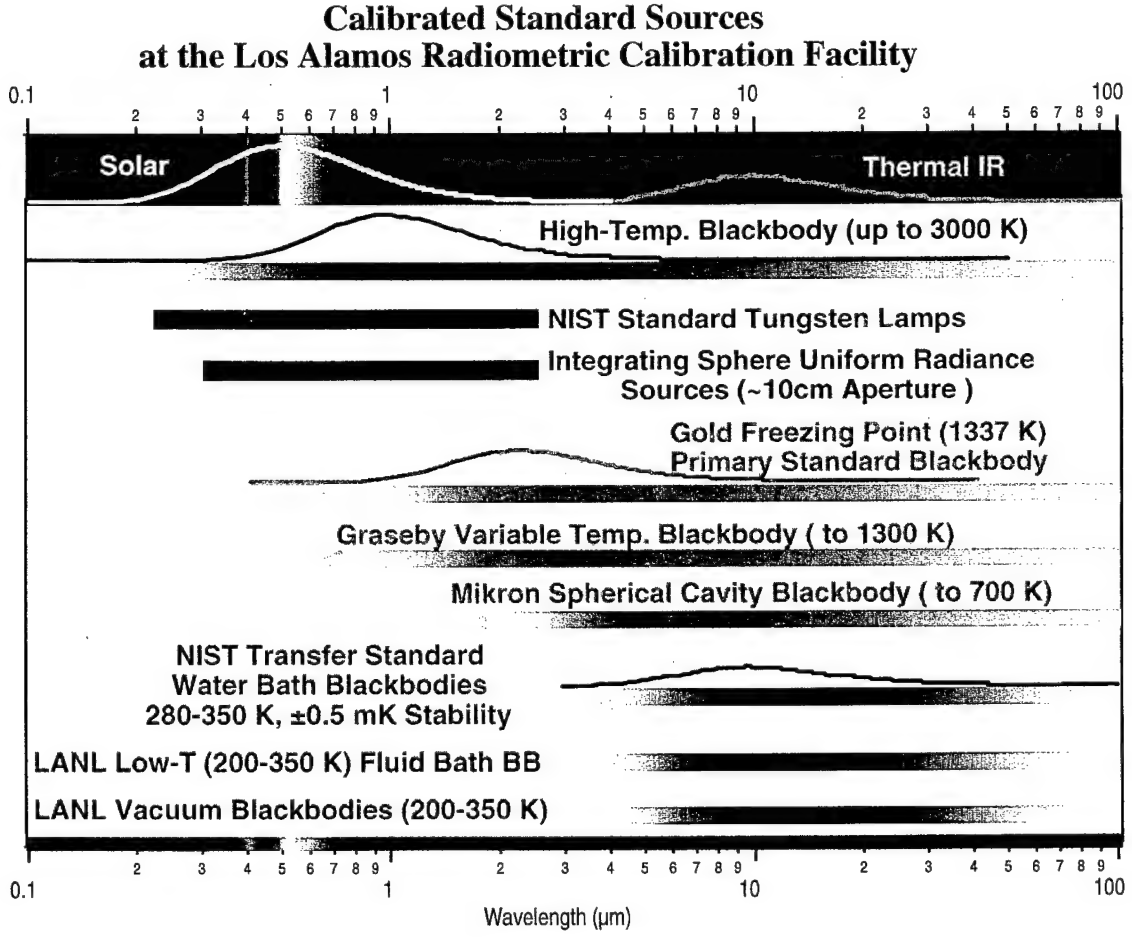

• Figure 20.

with 17 other absolute cavity radiometers. (3) A NIST-designed and calibrated Si composite bolometer, with spectral calibration from 2 to 15 μm at an accuracy of 1.4%. (4) Silicon trap photodiodes with NIST spectral radiometric response calibration better than 1% (3σ) over the 0.35 to 1.1 μm range and 0.33% (3σ) in the 0.4-0.9 μm range. (5) Commercial (LaserPrecision) pyroelectric radiometers. In addition, several other high quality IR detectors are in the calibration laboratory's inventory. Also available are calibrated InSb and HgCdTe infrared cameras. LANL detectors are summarized in Figure 21.

Tasks performed for SERDP:

Cavity Radiometer Intercomparison

Eighteen electrical substitution absolute cavity radiometers simultaneously measured the direct-beam solar irradiance from the same location, over a period of several days in October, 1994. This work tied the calibration of each of the participating radiometers to both the ARM program CART site

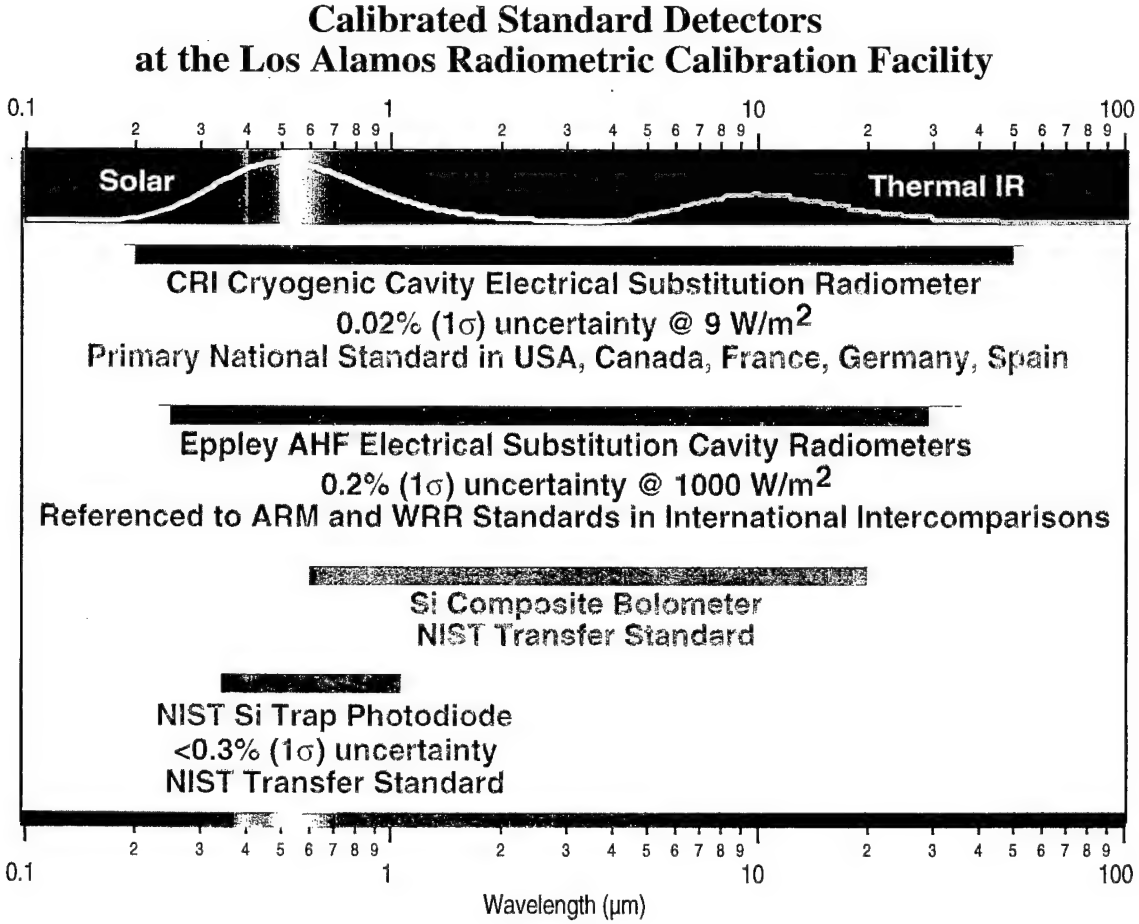

• Figure 21.

reference set, and (through the participation of the NREL/NOAA reference radiometers, recently returned from the World Radiometric Intercomparison in Davos, Switzerland) to the World Radiometric Reference. Absolute calibration of the radiometers is now known to within 0.1%, with respect to the World Radiometric Reference.

Pyrgeometer Round-Robin

Six Eppley pyrgeometers were calibrated by a variety of methods at twelve standards laboratories around the world, including LANL, NREL, NOAA, the Eppley Laboratory, the World Radiation Center in Switzerland, and national meteorological and standards laboratories in Canada, Australia, the UK, Germany, and Japan. The aim was to establish the validity and degree of equivalence of the various calibration strategies used for these ubiquitous instruments. Calibration at Los Alamos utilized our NIST fluid-bath blackbody operating at a variety of temperatures from 5° up to 70° C. A method of radiatively heating and cooling the filter dome of these instruments was developed, allowing calibration of the dome emission contribution to the pyrgeometer output. Using this method, it was found that dome emission effects can contribute very substantially to the pyrgeometer output -- as much as 20 $Wm^{-2}K^{-1}$ of temperature difference between the filter dome and reference junction -- thus underlining the need for thorough calibration of dome effects for all such instruments. Current plans include return of the pyrgeometers to Los Alamos for spectral characterization of the filter domes.

SSP

Multiple calibrations of SSP were performed at Los Alamos over the course of the ARM-UAV program, beginning in the spring of 1995, again during fall and winter 1995-96 following the ARESE campaign, and most recently in the summer of 1996 following the Spring 1996 campaign at the CART site. Calibration tasks performed included: (1) characterizing, at multiple wavelengths, the quality of polarization and the polarization orthogonality of the two linear polarization channels; (2) complete mapping at 1 nm resolution of the relative spectral responsivity at each of the 107 encoded positions along SSP's circularly variable filter for each of SSP's four channels (two linearly polarized narrow field of view channels, unpolarized narrow field of view channel, unpolarized quasi-hemispherical flux channel); (3) absolute spectral response calibration at each wavelength for each of the four channels; (4) angular response calibration of the quasi-hemispherical flux channel at each wavelength; (5) calibration of the temperature dependence of the absolute spectral response. This involved construction of a custom variable-temperature environmental chamber for SSP, capable of temperatures as low as -80° C.

The next three figures pertain to the SSP calibrations: The photographs in Figure 22 and Figure 23 show the SSP, mounted on an angular translation stage in the process of absolute radiometric calibrations using a standard lamp and an integrating sphere. Figure 24 shows the absolute spectral response of SSP channel 3: note the overlapping and vignetting effects at the edges of the circular variable filters (CVFs).

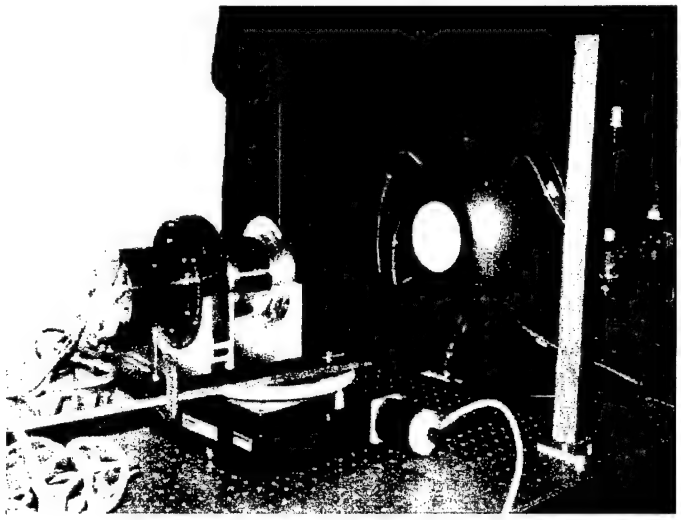

Figure 22. Integration sphere calibration of the SSP.

HONER

The Perseus B schedule delays precluded deployment of the HONER instrument. Thus completion of the HONER calibration was given lower priority than calibration of the other instruments. However, detailed calibration procedures have been developed and calibration will proceed when appropriate. Absolute calibration of the HONER shortwave sphere will involve intercomparison with electrical substitution radiometers, using both laboratory sources and the sun. The long-wave sphere will be calibrated using fluid-bath blackbody sources. Plans include characterization of the relative spectral responsivity over the entire spectral range of both spheres, including a coarse mapping of the difficult region beyond 20 μm using long-pass filters. In addition, nonlinearity, angular response, and equivalence of the up- and down-

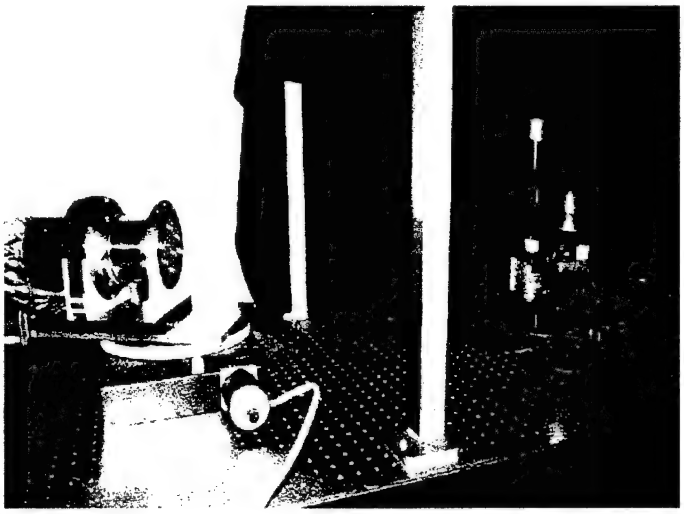

Figure 23. Standard lamp calibration of the SSP.

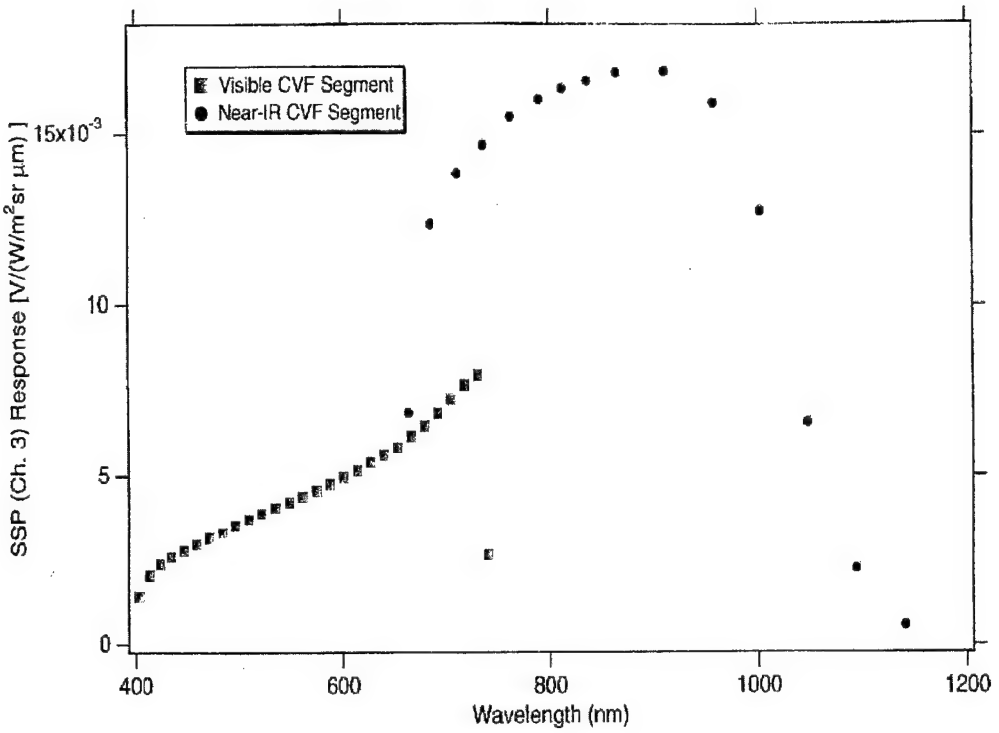

Figure 24. Absolute spectral response of the SSP unpolarized channel, as determined using the integrating sphere calibration source.

looking apertures of both units will be quantified.

MPIR

First Los Alamos calibration activity with MPIR was ground support during the Spring 1996 campaign. Upon delivery to Los Alamos, characterization of the four operational MPIR cameras revealed a latency / readout-rate mismatch in the near-IR arrays, leading to context-dependent nonlinear behavior, and a temperature-related responsivity drift in the Si cameras. Nevertheless, spectral characterization of all four channels was performed, within the nonlinear and drift limitations, and an absolute calibration and spatial flat-fielding of the Si cameras was performed. Once a fully functional MPIR is available, LANL is prepared to perform as full a calibration as schedule and funding allow. This would include spectral characterization of each channel, absolute responsivity calibration, and temperature-dependent responsivity characterization, especially of the LWIR channels. For this latter task, a custom environment chamber, capable of simulating both the temperatures and temperature gradients experienced on the aircraft, was specially constructed at Los Alamos.

AERI Fourier Transform Infrared spectrometer

The AERI-UAV FTIR instrument, being built by the University of Wisconsin, is only now being completed, and is therefore not available for calibration. Los Alamos has engaged in calibrations of two FTIR instruments for other programs, so the AERI-UAV activity will have a relatively short learning curve.

Summary

Los Alamos has established and improved their calibration capabilities, both by acquisition and development of hardware, and by working directly with NIST, NOAA, NREL and others to tie the calibrations to national and international standards. Hardware has been developed, built and tested and procedures established for calibrations of the ARM/UAV instruments. The actual calibration of the instrumentation was, of course, affected by instrument availability.

---

[1] Stephen H. Schneider, "The changing climate in managing planet Earth," readings from Scientific American Magazine, W. H. Freeman (1989)

[2] P. Pilewskie and F. P. J. Valero, "Direct observations of excess solar absorption by clouds," Science, **267**, 1626-1629

[3] Chester Wells, NREL, private communication

[4] Francisco P. J. Valero, Warren J. Y. Gore, and Lawrence P. M. Giver, "Radiative flux measurements in the troposphere," Appl. Opt., **21**, 831-38

[5] Philip D. Hammer, Francisco P. J. Valero, and Stefan Kinne, "The 27-28 October 1986 FIRE cirrus case study: retrieval of cloud particle sizes and optical depths from comparative analysis of aircraft and satellite-based infrared measurements," Mon. Weather Rev., **119**, 1673-92

[6] Y. Fouquart, J. C. Buriez, M. Herman, and R. S. Kandel, "The influence of clouds on radiation: a climate-modeling perspective," Rev. Geophysics, **28**, 145-66

[7] H. Hinterberger and R. Winston, "Efficient light coupler for threshold Cerenkov counters," Rev. Sci. Instrum. **37**, 1094-1095

Chapter

4

Measurement Technique Development and Initial Data

Clear Sky Profiling with UAVs - Fall 1993 and Spring 1994

Overview

The initial ARM-UAV flight series was known as the UAV Demonstration Flight (UDF). The objectives of UDF were to demonstrate the suitability of UAVs as a platform for scientific measurement and to obtain clear-sky flux profiles for comparison with atmospheric radiation transport models. The desired profiles are for both upwelling and downwelling fluxes for both solar radiation (0.4 to 4 μm, also called shortwave) and thermal infrared (4 to 30 μm or longer, also called longwave). In clear skies, fluxes change slowly with altitude, due to both reflection and absorption by atmospheric constituents; and both of these are strong functions of water vapor concentration and aerosol loading. In fact, the flux rate of change is slow enough that with the best instrumentation available, meaningful measurements can only be made for altitude differences of many hundreds of meters to a few kilometers in the lower atmosphere.

Aircraft and Instrumentation

UDF flights were conducted using the Gnat-750 UAV built by General Atomics Aeronautical Systems, Inc., shown in Figure 25. This UAV was chosen for the first flight series because it was a proven design with payload and flight characteristics suitable for the mission objectives. Its service ceiling allowed for measurements to 7 km.

Seven scientific instruments were mounted in the Gnat. The first five instruments were provided by Francisco Valero and his team at NASA Ames Research Center. A pair of matched shortwave broadband hemispherical radiometers were mounted such that one was pointing to the zenith and one nadir, measuring downwelling and upwelling solar radiation, respectively. Similarly a pair of matched longwave broadband hemispherical radiometers were mounted to measure downwelling and upwelling thermal radiation. The fifth instrument was a total direct diffuse radi-

ometer (TDDR) that measured downwelling radiation in seven solar bands from 0.38 to 1.6 μm. The TDDR has two external moving rings that periodically shade the radiation input port from direct solar radiation, allowing for the division of downwelling radiation into direct and diffuse fields. This division is important for the correction of downwelling shortwave broadband data for aircraft roll and pitch and for the determination of atmospheric aerosol loading. The sixth instrument was a Scanning Spectral Polarimeter, which measured upwelling solar radiation and its polarization in both 2π and 7 mrad cones from 0.4 to 2.4 μm with moderate spectral resolution (~90 bands). The last instrument was actually a suite of devices that measured in situ temperature and dew point. In addition to these scientific instruments, a GPS/INS system provided 10 Hz position and attitude data for use in the interpretation of the data from the other in-

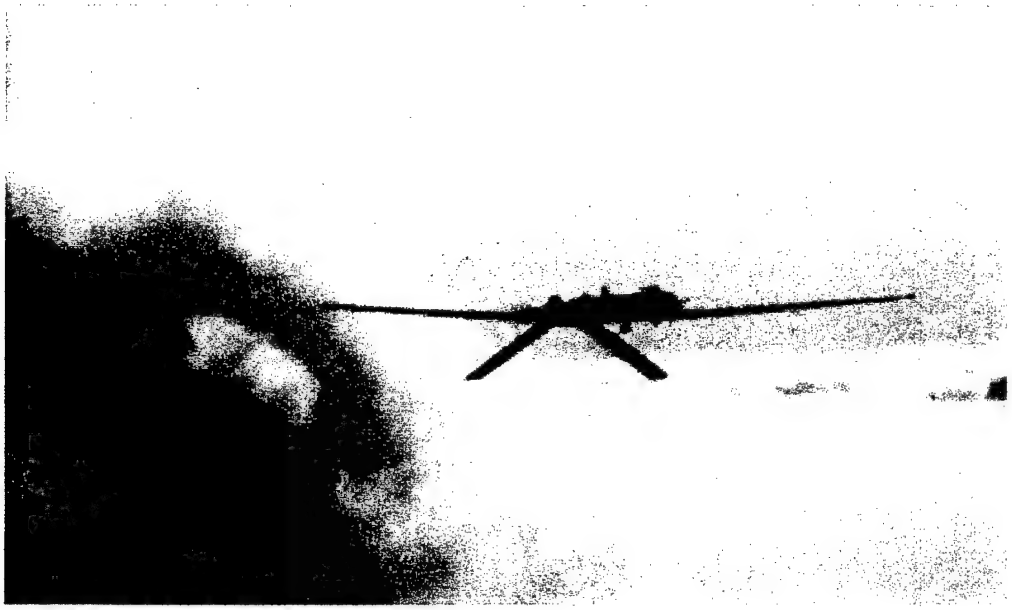

• Figure 25. General Atomics Gnat 750 over the CART Site in Oklahoma.

struments.

All data was telemetered from the Gnat to a ground station, where it was recorded for later decommutation. A small subset of data, called quick look data, was decommutated in real time and fed to instrument mentor stations in a collocated science trailer for their analysis of instrument performance. This field telemetry and data system is described in more detail in a later section. The mission scientist also performed a cursory analysis of the quick look data, and from this analysis was able to guide the conduct of the mission within general flight parameters to maximize the gathering of useful scientific data.

Flight Series

The first of the two phase flight series conducted in restricted air space at Edwards Air Force Base, California, in November, 1993. Although this was intended to be only an engineering flight to confirm that the payload and aircraft systems were functioning properly, such high quality data was collected for rare low aerosol and dry atmospheric conditions that it was subjected to scientific analysis.

The second phase was conducted in April, 1994, at the DOE Cloud and Radiation Testbed (CART) site in north central Oklahoma. The UAV flights were conducted from the small Blackwell Tonkawa general aviation airport 10 nm from the CART site. Since this was the first use of a UAV in non-restricted air space for scientific research, the FAA demanded that the Gnat be accompanied by a chase aircraft at all times. This restriction was later changed in subsequent series. An DHC-6 Twin Otter was used for chase. Vertical flux profiling was accomplished by flying the UAV at several altitudes up to 7 km over ground based radiometric instruments located at the CART site. The operation was supported by an intense observation period (IOP) at the CART site, including frequent balloon borne sonde launches for temperature and water vapor profiling.

Altogether approximately 22 hours of flight time was accumulated in nine flights that covered a variety of clear sky water vapor and aerosol conditions.

Data and Results

According to Dr. Francisco Valero (NASA Ames / Scripps), "radiation data of unprecedented quality were acquired demonstrating that UAVs are a very important platform for atmospheric radiation research. Successfully measuring accurate and unambiguous radiative flux divergence profiles in the clear atmosphere broke new ground from the scientific point of view. Flux divergence measurements are essential to test and validate atmospheric radiative transfer models and, thereby, general circulation models (GCMs). To achieve such results has been the dream of radiation scientists for decades."

Representative data from these flights are shown in Figure 26 and Figure 27. These figures compare measured (solid points) and calculated fluxes (solid lines) for both the solar and infrared portions of the spectrum. The solar calculations were performed by Dr. Koonan Liou (University of Utah) and contain no adjustable parameters; they use known albedos for spring wheat and aerosol optical depths as measured from the UAV. The longwave calculations were performed by Dr. Robert Ellingson (University of Maryland) using atmospheric state and surface measurements from the CART site. Except for the downwelling infrared, disagreements of a few

tens of Wm^{-2} are seen between the calculations and the measurements at selected altitudes.

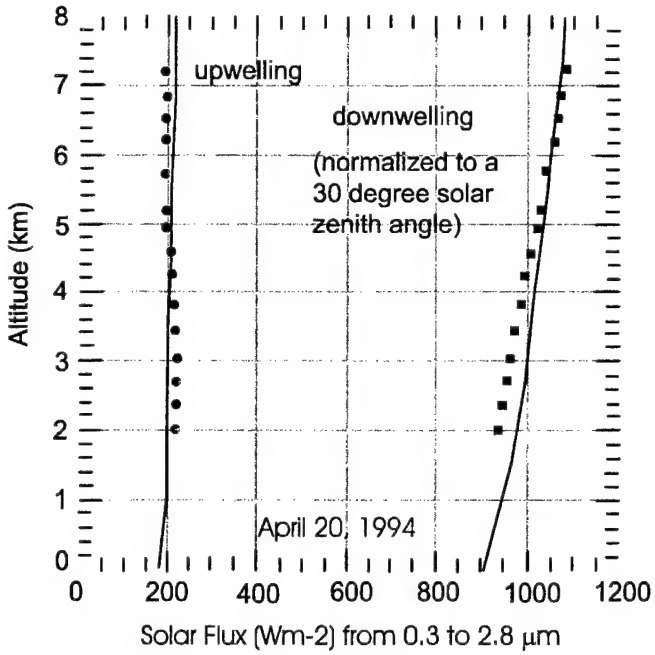

Figure 26. Solar calculations and UDF measurements.

Cloudy Sky Measurements with Coordinated Aircraft - Fall 1995

Overview

Measurements taken from several locations around the globe suggest that clouds may absorb significantly more energy than previously thought and represented in current climate models. The magnitude of this enhanced solar absorption appears to be on the order of 25-40 Wm-2. If true, this enhanced absorption would profoundly change how we understand the partitioning of solar energy between the atmosphere and the surface. Therefore, the ARM-UAV and ARM programs undertook the ARM Enhanced Shortwave Experiment (ARESE) in October and November, 1995.

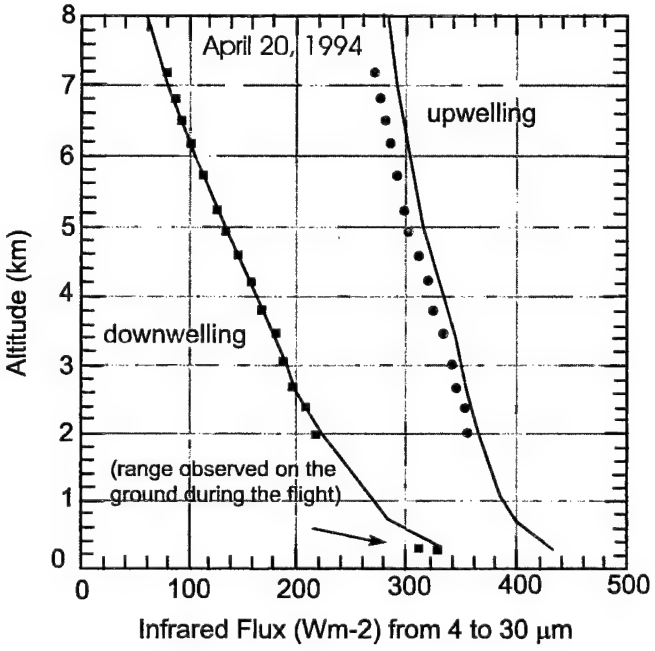

Figure 27. Infrared calculations and UDF measurements.

ARESE was a six week long campaign to test our understanding of the interaction of solar energy with clear and cloudy skies which

focused on two scientific objectives: (1) the direct measurement of the absorption of solar radiation by clear and cloudy atmospheres and the placement of bounds on these measurements, and (2) the investigation of the possible causes of absorption in excess of the model predictions.

Platforms and Instrumentation

To accomplish these objectives, ARESE used a combination of satellite, aircraft, and ground observations to make highly accurate solar flux measurements at different altitudes throughout the atmospheric column.

Because a UAV with the required characteristics was not available in time for ARESE, the Egrett, a piloted aircraft built in Germany by Burkhart Grob and shown in Figure 28, was used as the medium altitude (up to 45,000 ft) aircraft. The same instruments were incorporated into the Egrett payload as had been flown on the Gnat 750 (see page 53) with three exceptions. First, two fractional solar broadband hemispherical radiometers were flown in lieu of the two infrared broadband instruments. These were mounted in the same nadir and zenith manner as the ones they replaced, and covered the spectral band 0.7 to 3.0 μm. Secondly, a second TDDR, but without shadow rings, was mounted in a nadir viewing direction. Finally, the CDL made its debut at this time, mounted in a blister on the side of the Egrett where it could be rotated to view either in the ze-

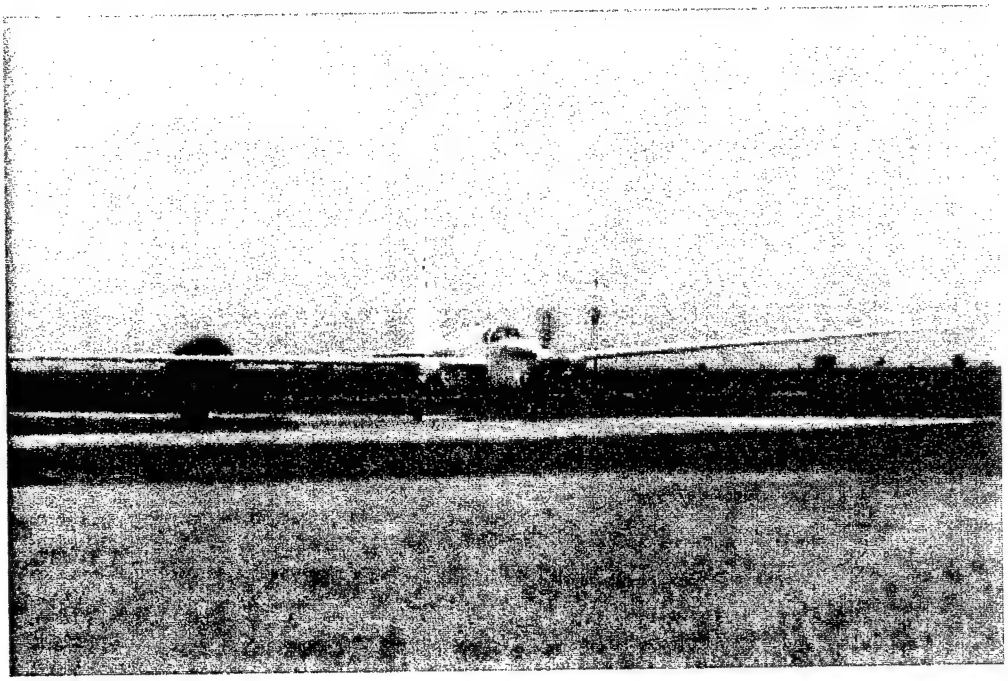

Figure 28. Grob Egrett with ARM-UAV payload preparing for takeoff.

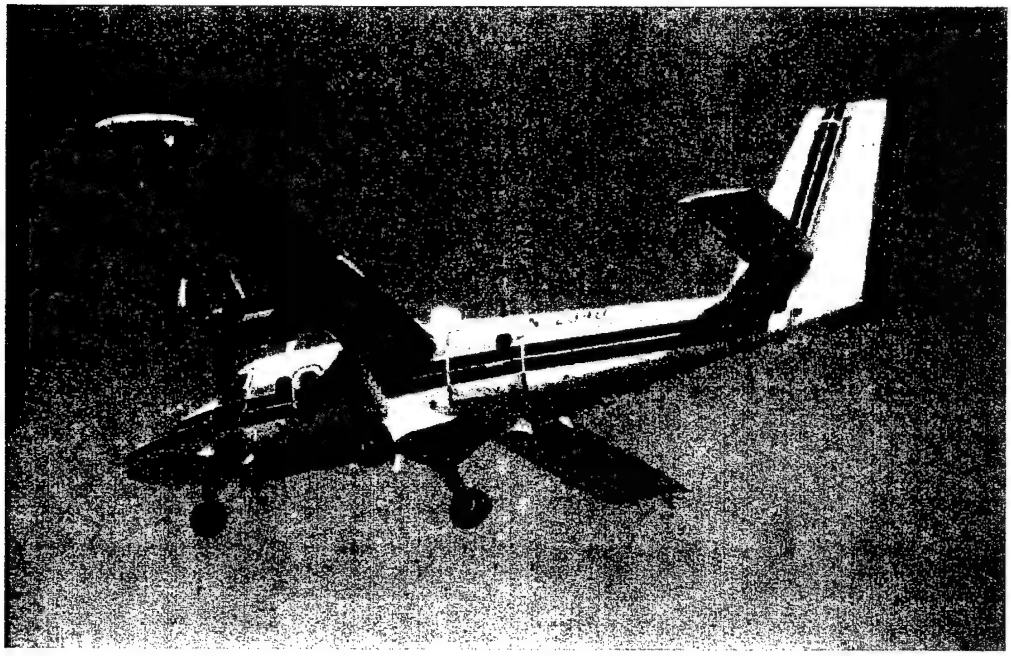

Figure 29. Instrumented Twin Otter used for UAV chase and as a science platform. Instrument turrets can be seen above and below the midsection.

nith of nadir direction.

A chase plane is usually required to escort the UAV in selected operating conditions. For this task, the ARM-UAV program normally uses a de Havilland Twin Otter (DHC-6), which can match the UAV's air speed envelope. ARM-UAV has taken advantage of this chase plane by mounting instruments on it so that it can serve as the second aircraft in experiments requiring simultaneous measurements above and below cloud layers when not needed for chase operations. For this campaign, the Twin Otter carried a radiometric set matched to the solar broadband, fractional solar broadband, and TDDR instruments on the Egrett, as well as an in situ meteorological package that measures temperature and dew point. A picture of the instrumented Twin Otter is shown in Figure 29. The band passes of the seven channels on the TDDRs on both the Twin Otter and the Egrett were adjusted to optimally support cloud studies.

The other critical elements in this experiment, but elements not directly funded by SERDP and ARM-UAV, were the GOES-8, NOAA-12, and NOAA-14 satellites, an ER-2, and the CART site. A radiometric set matched in performance to those carried by the Egrett and Twin Otter was carried by the ER-2 and three similar sets mounted on the ground in the extended CART site area. Many of the ground instruments that form the normal complement at the CART site, as well as some ground based

cloud radars specially deployed for this experiment, were used to complete the needed scientific data set.

Flight Series and Stacked Aircraft

The baseline ARESE flight were conducted at the CART site from September 25 through November 1. During that time twelve scientific data flights were flown that accumulated approximately 60 hours of in flight data under a variety of atmospheric conditions ranging from clear to solid overcast. One of two ground tracks, shown in Figure 30, was selected by the science team prior to each flight based on projected cloud conditions; these tracks were sufficiently long (>100 nm) to ensure good coverage of the normal variability of conditions in a cloud layer, and to ensure good statistics in the flux averages over these conditions. Table 7 shows a summary of the flights made in the campaign.

The key to ARESE was a carefully "stacked" Twin Otter and Egrett "cloud sandwich". The vertical stacking of the aircraft was accomplished by a system developed by ARM-UAV based on global positioning systems located in each aircraft that communicated and displayed the position of

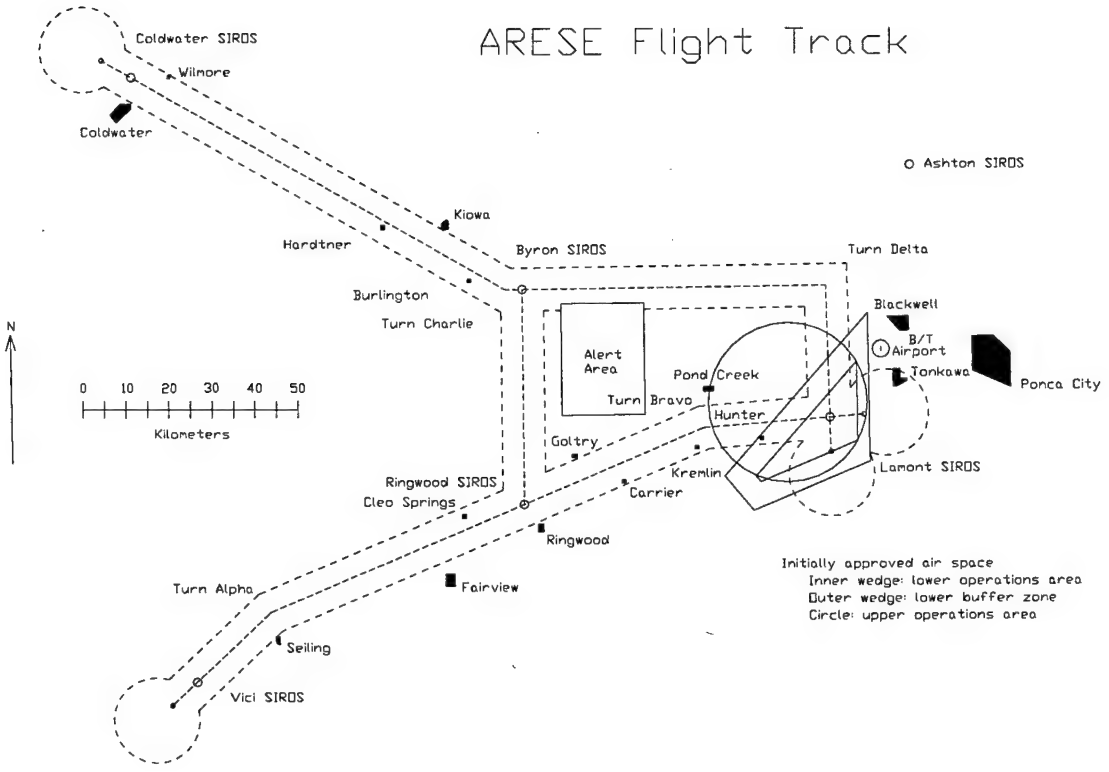

Figure 30. ARESE northwest and southwest flight tracks.

both aircraft relative to each other and to the desired flight track. Using this system, the pilots were able to control the horizontal position of their aircraft to within 100 meters or so while separated by approximately 12

• Table 7. Campaign Summary for Fall 1995

Date in 1995	*Aircraft*	*Conditions*
Sept 25	Egrett, Twin Otter, ER-2	Solid to broken cloud field along NW track
Sept 29	Egrett, Twin Otter, ER-2	Scattered to broken clouds, lots of turbulence
Oct 3	Twin Otter, ER-2	Clear sky profiling at 4, 7, 10, 13, 16, 19 kft; albedos at central facility
Oct 11	Egrett, Twin Otter, ER-2	Clear sky albedo, column absorption, and inter-comparison
Oct 13	Egrett, Twin Otter	Cloudy sky absorption on NW track (alto stratus and cirrus)
Oct 17	Egrett, Twin Otter, ER-2	Clear sky mission, data inter-comparison on SW and NW legs
Oct 19	Egrett, Twin Otter, ER-2	Clear sky albedo, column absorption NW leg
Oct 24	Egrett, Twin Otter	Thin cirrus cloud field
Oct 26	Egrett, Twin Otter	Sold cirrus deck to broken clouds to clear sky
Oct 28	Twin Otter	Clear sky, Otter only experiment at 500 ft above Charlie Whitlock's radiometers to explore aerosol heating -- also excellent albedo data
Oct 30	Egrett, Twin Otter	Thick uniform low to mid-level deck
Nov 1	Egrett, Twin Otter	Solid to broken cloud field

km in altitude.

During ARESE measurement flights, the Otter was generally flown at 0.5 km above ground level and the Egrett at 13 km. This pair of stacked aircraft was over flown by an ER-2 flying at 20 km, which because of its much higher speed did not stay in constant alignment with the Twin Otter and Egrett stack but did provide periodic coincidences with these other aircraft.

Radiance measurements from the GOES satellites were used to retrieve top of the atmosphere fluxes. These flux measurements were supplemented by a variety of cloud property measurements from the ground, the Egrett, and the ER-2, including radar, LIDAR, and multispectral measurements.

Data and Results

Atmospheric conditions remained abnormally clear for most of the campaign, but there were enough cloudy days, especially in the first part of November, to allow flights and data gathering under a variety of atmospheric conditions ranging from clear to solid overcast.. These flights included: cloud forcing experiments under scattered, broken, and solid overcast conditions including low, mid and high level cloud decks; clear sky column absorption and surface albedo measurements; clear sky flux profiling measurements; and in flight coaltitude intercomparisons of flux measurements made from the two aircraft. The data have just been released to the broad scientific community in June, 1996, and are of excellent quality, especially considering that all three aircraft carried identical up and down looking radiometers and flew over identical up looking radiometers at the CART central and extended facilities. The data comprise a unique set for testing our understanding of the absorption of solar radia-

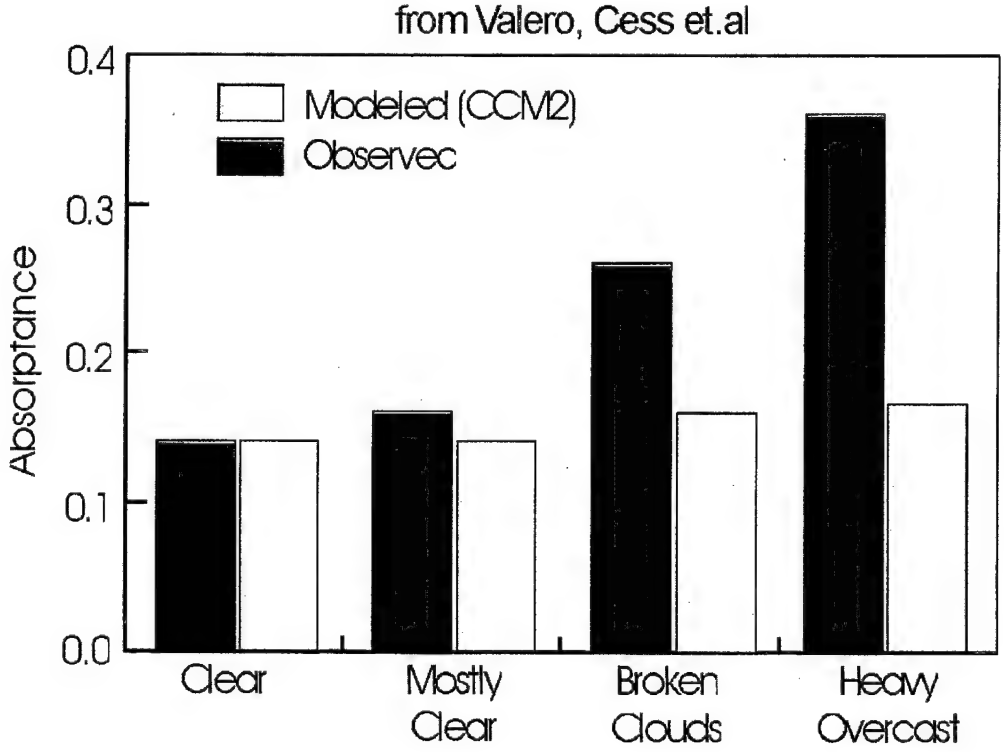

Figure 31. Cloudy atmosphere calculated versus measured absorptance.

tion in both clear and cloudy atmospheres, and analysis is ongoing. Early results indicate that cloudy skies do indeed absorb more shortwave radiation than predicted by current models. An example of an analysis by Valero and Cess is shown in Figure 31

Experiments with the New UAV Instruments - Spring 1996

Early in calendar year 1996, the development of some of the new UAV instruments was nearing completion. These instruments made possible a variety of new experiments as proposed by the ARM-UAV Science Team. These experiments were developed and described in the ARM-UAV Science and Experiment Plan:; 1996 Flight Series[i]. The titles for the fourteen experiments contained in that document are shown in Table 8.

• Table 8. ARM-UAV Planned 1996 Experiments

Number	*Title*
1	Satellite narrowband calibration
2	Satellite narrowband radiances to TOA fluxes
3	Effect of scale on retrieving cloud properties
4	Three dimensional cloud effects
5	Cloud observation distance
6	ARESE reprise
7	Cloud microphysics from various sensors
8	Cloud Water Phase distribution
9	Cirrus cloud optical properties
10	Bi-directional reflectance functions
11	Diurnal radiation budget quantities
12	Contrail impact on the local radiation field
13	Water vapor absorption
14	Clear sky profiling with aerosol sampling

Unfortunately, during the winter of 1996 the UAV provider flight schedules for both the Perseus B and Altus (then known as the "High Altitude Test Bed") had slipped beyond supporting a spring flight series. Therefore, an April, 1996, campaign was undertaken using the same two aircraft used in ARESE (the Egrett and the Twin Otter), but now with the Egrett flying the newly developed frost point hygrometer and MPIR (although the MPIR only had mounted the 0.62-0.67 μm, 0.86-0.90 μm, 1.36-1.39 μm, and 1.58-1.64 μm modules) as well as the standard radiometric, SSP, and in situ payload. Also the CDL, which had made its maiden flight on the Egrett during ARESE, was flown again. The Twin Otter payload was now augmented with a Microwave Radiometer, an instrument useful

in determining the liquid water content in clouds above the aircraft. This combination of aircraft and instruments allowed all the experiments in the Science and Experiment Plan to be conducted, except Experiment 11, which required UAV long endurance capability, and Experiment 13, which required the UAV-AERI.

Seven science flights were made over a period of three weeks in April and May, 1996, as shown in Table 9. Four of these involved stacked flight, as discussed previously on page 53. Of the twelve possible experiments, eight were flown. Many of these experiments require a wide range of meteorological conditions, and will have to be repeated on future campaigns as additional conditions present themselves to broaden the acquired data set.

The flights on May 3 and May 4 were flown in conjunction with the Sub-

• Table 9. Campaign Summary for Spring 1996

Date in 1996	*Aircraft*	*Experiment and Conditions*	*Experiment Plan Numbers*
Apr 18	Egrett	Clear sky GOES-8 calibration Clear sky NOAA-14 calibration Clear sky BDRF measurement	1, 2, 10
Apr 20	Egrett, Twin Otter, DC-8, ER-2	Cirrus optical properties; SUCCESS in situ sampling Cirrus microphysics Cirrus SSP BDRF measurement Profiling through cirrus deck	7, 9, 10
Apr 27	Egrett, Twin Otter	Cirrus microphysics Light cirrus NOAA-14 calibration Cirrus BDRF measurement	1, 7, 10
May 3	Egrett, B757, T-39, DC-8, ER-2	Clear sky NOAA-14 calibration Clear sky contrails Clear sky BDRF measurement	1, 2, 10, 12
May 4	Egrett, Twin Otter, B757, T-39, DC-8, ER-2	Stratus GOES-8 calibration Stratus NOAA-14 calibration Stratus BDRF measurement Stratus geometry; two aircraft over clouds Stratus geometry; aircraft over and under clouds Broken sky contrails	1, 2, 4, 5, 10, 12
May 5	Egrett, Twin Otter	Broken cumulus GOES-8 calibration Broken cumulus geometry; aircraft over and under	1, 2, 4
May 6	Egrett	Calibration of C-MIGITS and RAMS against the sun	N/A

sonic Aircraft: Contrail and Cloud Effects Special Study (SUCCESS), a major NASA experiment studying the impact of aircraft on local climatology. The SUCCESS experiment fielded four aircraft equipped with a wide range of in situ aerosol and remote sensing instruments: an ER-2, a B-757, a DC-8, and a T-39. Positioning these aircraft with the ARM-UAV aircraft for the conduct of Experiment 12 "Contrail Impact on the Local Radiation Field" proved to be very difficult using voice relayed GPS coordinates and checkpoints.

Data from this campaign will form a rich data set; it will be released in January, 1997, after being reviewed and calibrated by the various instrument PIs.

Geostationary Satellite at the Tropopause with the Altus - Fall 1996

In September, a preliminary version of the General Atomics Altus UAV finished development testing and became available for deployment on a scientific campaign; Figure 32 shows Altus deployed to the Oklahoma campaign site. In this campaign, the scientific objectives laid out in the Science and Experiment Plan which guided the Spring 1996 campaign were pursued further to expand the range of meteorological conditions

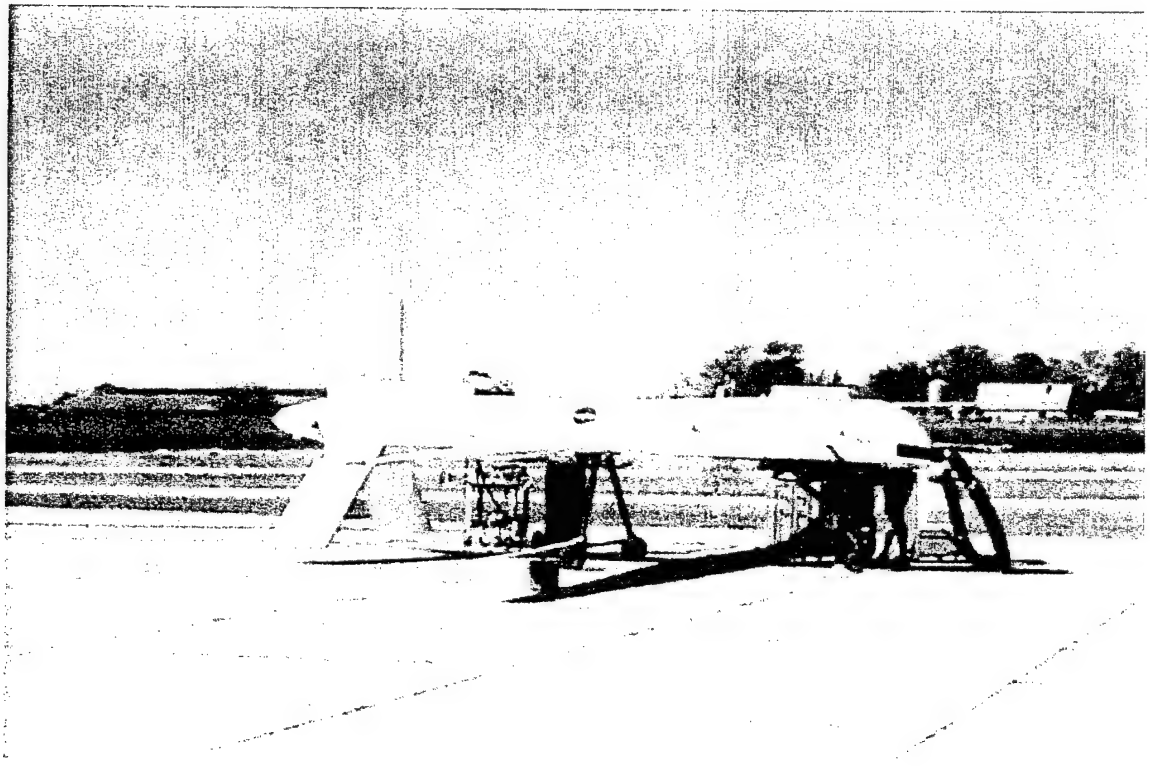

Figure 32. Altus UAV on the ramp at Blackwell Tonkawa Airport. The black hoses at the front provide chilled air to the payload prior to flight.

• Table 10. Campaign Summary for Fall 1996.

Date in 1996	*Aircraft*	*Experiment and Conditions*	*Experiment Plan Numbers*
Sept 17	Twin Otter	Over and under stratus deck with clear above	4
Sept 20	Twin Otter	Water vapor IOP support	N/A
Sept 24	Twin Otter	Water vapor IOP support	N/A
Sept 27	Twin Otter	Water vapor IOP support, night flight	N/A
Sept 29	Altus, Twin Otter	Clear sky GOES-8 calibration Clear sky BDRF Clear sky MWR calibration turns RAMS Intercomparison Clear sky profiling (modified Experiment 14)	1, 2, 10, 14
Sept 30	Altus, Twin Otter	Clear sky MWR calibration turns RAMS Intercomparison	N/A
Oct 3	Altus, Twin Otter	Clear sky GOES-8 calibration Clear sky BDRF Clear sky MWR calibration turns RAMS Intercomparison Clear sky profiling (modified Experiment 14)	1, 2, 10, 14
Oct 4-5	Altus, Twin Otter	Diurnal flight - 24 hrs, 46 min on station Clear sky GOES-8 calibration Clear sky NOAA-12 calibration Clear sky BDRF RAMS Intercomparison Clear sky profiling (modified Experiment 14)	1, 10, 11, 14

under which data was taken.

The payload developed for the Altus included all the instruments carried by the Egrett, although payload bay configuration limited the CDL to only nadir viewing. Infrared broadband radiometers were substituted for the fractional solar radiometers to permit important analyses of longwave fluxes. Total weight restrictions allowed only two of the three instruments in the set of CDL, MPIR and frost point hygrometer to be flown at one time. However, a reasonably quick reconfiguration capability in the field for the payload ameliorated this limitation and allowed the payload suite to be matched to the selected experiments prior to any flight.

As configured, the Altus had a service ceiling in excess of 11 km, well above the FAA Class A (instrumented aircraft only) airspace lower limit.

This made possible the first ever use of a unescorted UAV in civilian airspace for scientific research. After discussions with the FAA regional representatives, a radio relay system was added to the Altus, and approval was granted for unescorted flight above 18,000 ft. All UAV flights in this campaign thus involved chase plane escort to this altitude, UAV IFR (instrument flight rules) flight above, and then chase plane escort back to the Blackwell Tonkawa airport.

Eight science flights were made in this campaign between September 17 and October 5, 1996. A summary of the flights and their objectives is shown in Table 10. Four of these involved stacked flight, as discussed previously on page 53. Of the fourteen experiments listed in the Science and Experiment Plan, it was possible to fly twelve with the aircraft and payload configurations available. Experiment 12 and the full Experiment 14 involved cooperation with the SUCCESS aircraft and could only be flown concurrently with that experiment in Spring, 1996, and Experiment 13 required the UAV-AERI. A modified Experiment 14 was flown, however, that incorporated clear sky profiling without aerosol sampling. Of the twelve possible experiments, six were flown, adding diversity to the data set from the Spring 1996 campaign.

Of particular interest is the fact that the availability of the Altus, with its long endurance capability made Experiment 11 possible, Diurnal Radiation Budget Quantities. On the last flight, the Altus was flown for 26 hours, 11 minutes from wheels up to wheels down, with 24 hours and 46 minutes of on station time. Actual fuel loading would have permitted an additional 6 hours of flight.

Data from this fall campaign will be released along with data from the spring campaign in January, 1997, after being corrected by the various instrument PIs.

---

[i] Robert Ellingson and Tim Tooman, eds., ARM-UAV Science and Experiment Plan; 1996 Flight Series, Revision 4, March 2, 1996

Chapter

5

Data Management and Release

Telemetry System

The application of telemetry allows the instrument mentor to obtain real time science data during flight with the advantage that the science mission and flight parameters may be modified while the UAV is airborne should atmospheric conditions change. Telemetry also allows the instrument mentors to monitor the status of their instruments and to power them down if necessary. For a single instrument, this prevents possible sensor damage in off normal operating circumstances and allows the flight to continue with the rest of the payload operational.

Airborne Component

A flexible telemetry system was developed for the ARM-UAV program and it's applications whether on a UAV or manned aircraft. This system is designed to support both the current science instrumentation suite and capable of expansion for new (yet to be defined) science instruments. It is capable of operation on an unpressurized aircraft at an altitude of 20 Km with flight duration of 72 hours.

The flexible telemetry is a 1 Mb/sec. (3.0 MHz bandwidth) PCM/FM modulated, NRZ formatted system. Information is transmitted to a ground receiving station (no data is presently stored on-board) and via an up-link, operational commands may be passed on to the science payload. In an effort to make this telemetry system adaptable, extensive use of commercial hardware was employed and only a few selected circuit boards were custom designed.

The telemeter system consist of 5 major sub system chassis: ITP, PCS, PDS, DC/DC Power Supplies and Transmitter. Power for the telemeter system is supplied by the aircraft's +28 V DC generator

Sub Systems

Integrated Telemetry Processor (ITP) - The ITP collects the majority of the instrument data and formats all telemetry information for down link transmission. The format information is contained in EPROM memory and

is preprogrammed to comply with the instrumentation suite for each particular deployment. Collected data includes all science and diagnostic signals. This data may be either digital (both serial and parallel) or analog; no processing of the sampled data is done by the ITP.

PC-Controlled Subsystem (PCS) - The PCS controls all instruments and Power Distribution Systems. It is commanded by it's own internal 80486 microprocessor. Aircraft attitude data is generated by an on-board INS/GPS system that communicates with the telemetry system via a RS-232 serial link. However, this information is not in a form acceptable for telemetry; it must de-packetized, converted from floating point numbers, and processed. This is accomplished within the PCS system and then the INS/GPS data are imbedded into the down linked data stream. The balance of data is collected within the ITP sub system. Commands to the PCS are received via a second RS-232 serial stream generated by the UAV's on-board computer. This information must also be de-packetized and processed prior to command issuance.

Power Distribution System (PDS) - The Power Distribution System (actually comprised of two identical units) distributes, filters and fuses the +28 VDC aircraft supplied power for the instrumentation suite and subsystems in the payload. Each PDS has six filtered and switchable output ports and six unfiltered and switchable output ports. There are also two filtered outputs that are not switchable. Filtered outputs are capable of 6 A each, the unfiltered can supply 10 A each. Commands generated by the PCS powers on and off the science instruments, heaters, fans, etc. by utilizing the switching capability of the PDS.

DC/DC Power Supply - The flex telemetry has voltage requirements other than +28 VDC as supplied by the aircraft. The DC/DC power supply is a module containing three 30 W regulated voltage converters to supply the necessary power. These voltages differ as to the subsystem and are in the form of ±12 V, ±15 V and +5 V.

Transmitter - Data is down-linked via a 4 W E-band transmitter operating at a frequency of either 2205.5 or 2235.5 MHz depending upon the transmitter selected. Bandwidth is filtered via a six pole Bessel Hybrid located in the ITP to minimize harmonics and maintain 3 MHz bandwidth at the -3dB point.

Data

The UAV telemetry is capable of collecting multiple digital and analog streams from each instrument. This data may be synchronous or asynchronous in nature. The instrumentation suite deployed on the Altus UAV in the Fall of 1996 had the science and diagnostic inputs and sample

rates shown in Table 11. While not all diagnostic measurements were conducted, the appropriate channels were available if required.

Digital - Digital data interfaces may be either serial RS-232, RS-422, EIA-530, or parallel. While 8-bit parallel data is preferred, up to 24 bits has been accommodated. Maximum digital data sample rate is dependent upon the total complement of science instruments. In the present configuration, one instrument is generating information at 79.3 kB rate from a synchronous serial stream.

Analog - Analog data can be digitized to 8 bits at a rate of up to 10 kHz; the maximum rate for 12 bit conversion is 2 kHz.

Uplink Command Structure

The UAV telemetry has the capability to provide commands to the instrumentation suite while airborne Uplink commands to the PCS sub system

• Table 11. Flexible Telemetry Input for Altus at the Fall 1996 Campaign

Data Type	*Number of Channels*	*Type*	*Data Rate*
Science instrument	2	16 bit parallel digital	10 Hz
Science instrument	4	24 bit parallel digital	10 Hz
Science instrument	30	Analog to 12 bit	10 Hz
Science instrument	6	Analog to 8 bit	10 Hz
Science instrument	1	RS-232 serial	9.6 kbps
Science instrument	1	RS-232 serial	19.2 kbps
Science instrument	1	EIA-530 synchronous serial	79.3 kbps
Science instrument	1	RS-422 serial	19.2 kbps
Science instrument	1	9 bit FIFO memory	5.2 kHz
Diagnostic + voltage	102	Analog to 8 bit	10 Hz
Diagnostic - voltage	30	Analog to 8 bit	10 Hz
Diagnostic temperature	48	Analog to 8 bit	10 Hz
New instrument	1	RS-232 serial	9.6 kbps
New instrument	1	RS-232 serial	150.0 kbps

are originated on a laptop computer and via a RS-422 serial stream routed to the UAV's control facility. Here the commands are imbedded into the UAV's flight control data command link. The UAV's on-board computer channels this information by RS-232 serial link to the flex telemetry. When operated onboard a manned aircraft a RF modem system is substituted for the UAV command uplink to allow for payload uplink commands.

There are three major implementations of uplink capabilities: First, eight different discrete control signals can be routed to each instrument to turn it on or off, change its sensor gain, etc.. These signals are translated in the PCS sub system and converted to TTL logic. Next, the telemetry has the capability to independently switch on or off the +28 V DC to each instrument at the PDS. Finally, there also is a capability to issue serial RS-232 commands to each instrument.

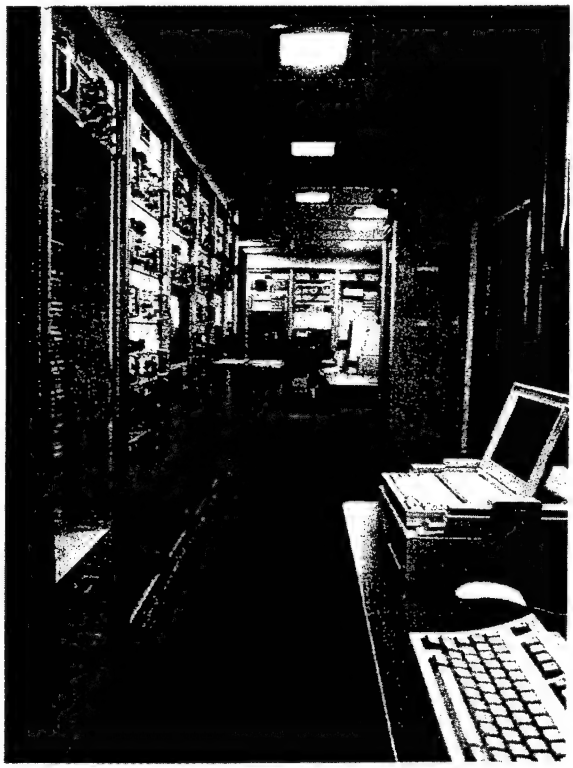

• Figure 33. View inside the Payload Ground Station Trailer.

Payload Ground Station

Overview

The primary objectives of the Payload Ground Station (PGS) are: (1) to receive the RF transmissions from one or two airborne platforms, (2) record the resultant raw data streams, and (3) preprocess the raw data streams into a suitable form for scientific manipulation. Important secondary capabilities include (1) the display of real time payload state-of-health including selected diagnostic measurements and (2) the dissemination of quick assessment science data to instrument mentors, as discussed on page 73.

The PGS is configured as a recording and data processing facility receiving input from up to two automatic RF tracking antennae. The recording station is a mobile 40 ft self contained, air-conditioned trailer. All equipment including antennae controls are maintained inside this facility. A view inside the trailer is shown in Figure 33.

Subsystems

RF Receivers - Four wide band receivers are available to acquire raw data from the tracking antennae. Two receivers are normally used for each aircraft, thus the ability to acquire data from two aircraft is possible when two tracking systems are deployed. Another pair of receivers are employed by the tracking antennae themselves as control to follow the aircraft in flight.

Recorders - Four 8mm digital tape recorders are incorporated within the PGS. Recording time is dependent upon the telemetry data rate with nominal 6 hours per tape for a 1 Mb / Sec. telemetry. During flight, two recorders are used to collect the raw data with one as primary and the second as backup. If two aircraft are airborne at the same time, one recorder is dedicated to each aircraft and a third used to record both aircraft down linked data streams. On extended flight missions, the fourth recorder is set up to start recording prior to the primary recorder reaching end-of-tape. This allows over lap of data so that no information is ever lost due to change of tapes. The information recorded includes raw telemetered data, IRIG time code, and all voice communication between the mission scientist, mission controller, flight crews, telemetry crew, and ground crew.

Time Code - A time code receiver acquires GPS signals and generates IRIG "B" data that is used to correlate data on the tape to the GPS time imbedded in the down linked data stream.

Decommutation System - Reproducing data from the telemetered PCM format is handled within the Quad-7 system. This hardware reformats the down linked data into the manner it was introduced to the telemetry system. Individual data words are tagged and via ethernet made available for mentor's quick assessment of their instrument. Working in conjunction with a work station, netCDF files for each instrument are generated to 8mm tape. The generation of data files is conducted real time while the aircraft is airborne. The file tapes after a flight are forwarded to Pacific Northwest National Laboratory (PNNL) for quality checks.

Work Stations - Work stations are part of the facility. They allow telemetry personnel to view all payload diagnostic data during a flight.

Tracking Antennae - The tracking antennae are dual axis systems that are normally operated automatically or may be manually controlled. Two wide band receivers control an antenna. The radio frequency (RF) signal is passed through a combiner which selects the best signal (either vertical or horizontal polarized) and routes the RF to the data receivers. A video camera with a long range zooming telescopic lens is mounted on each antenna to visually track the aircraft. This information is recorded with a VCR recorder. One of the antennae is shown in Figure 34.

Transceivers - A complement of hand held and rack mounted VHF radio transceivers, scanners etc. are part of the facility and are used to communicate with other campaign personnel.

On-Site Data Management System

The on-site data management system consists of several computers linked to each other, the Payload Ground Station, and the Internet. This system cooperates to collect, re-distribute, and display data in support of the UAV mission. Key elements of the system are displays for the mission controller, mission scientist, instrument mentors, collaborating scien-

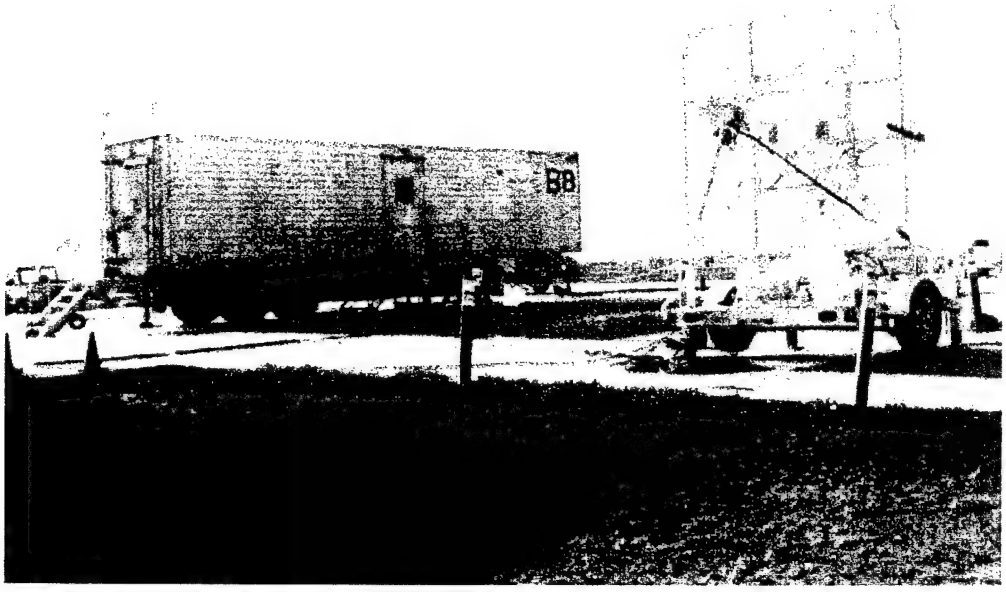

Figure 34. Malibu Tracking antenna on site in Oklahoma in front of the PGS trailer.

tists, and technical support. The primary purposes of the system are to aid in mission and science planning and analysis as well as to monitor the status of the airborne instruments and payload. Figure 35 is a schematic of the network architecture; Figure 36 shows the Helios and Mercury computer stations inside the science trailer.

Mission Aircraft Quick Look

The UAV quick look data is forwarded from all mission aircraft by the payload ground station in real time via network to the primary quick look computer in the science facility. In some cases, the quick look data is subsampled to reduce the real time computing load in the payload ground station. The primary quick look computer prepares the data for display and distributes the data to the instrument mentor computers. It also provides displays for the mission scientist, mission controller, and technical support to aid in analysis of the scientific data, in aircraft flight coordination

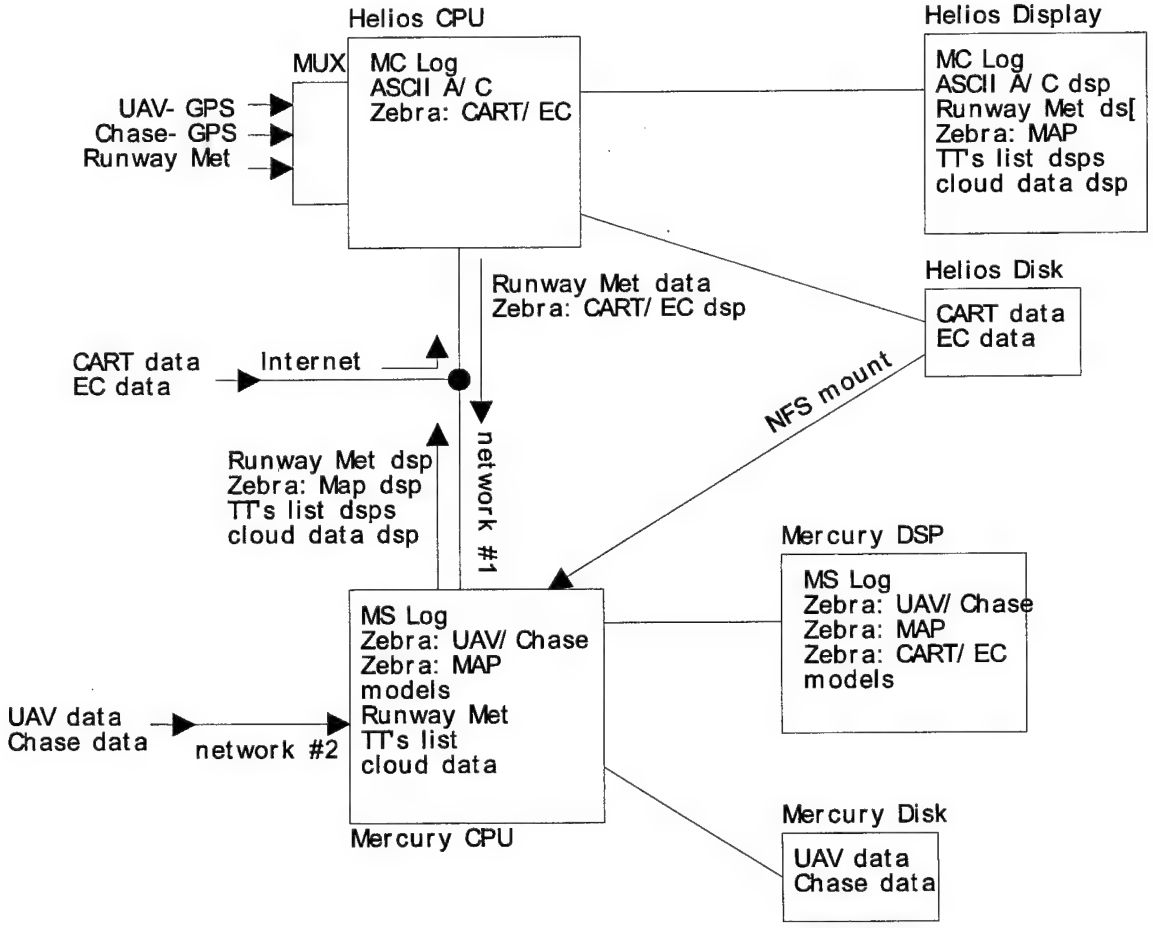

Figure 35. During a flight data is transmitted via ethernet among several computers for use by the Mission Scientist and instrument mentors.

Figure 36. View inside one half of the science building at the Blackwell Tonkawa Airport showing some of the mission computers and stations.

and control, and monitoring of the payload and instrument status.

The aircraft quick look data is shared via network with the instrument mentors. The quick look data allows the scientists to monitor instrument status as well as to preview the data with approximate calibration factors to assess the data quality. This capability coupled with the uplink equipment described below allows the instrument mentor to alter the state of an instrument to either improve performance or safeguard the instrument. This capability has improved overall capability to identify and possibly correct payload system or instrument problems on the spot.

Science and Operations Tools

The mission scientist and controller are provided tools to aid in science and operations planning, record keeping, communications, and payload adjustment. The tools have access to data from a number of sites at the nearby Southern Great Plains (SGP) Cloud and Radiation Testbed (CART) as well as other data sources.

Meteorological data is collected frequently and around the clock from various sites and agencies including the National Weather Service, selected SGP CART sites, and the UAV airport. This data is displayed in near real time to assist in scientific as well as flight controller decisions influenced by current weather conditions. Satellite images are collected

and displayed for additional weather tracking. Internet connection to national expert meteorological systems is also available.

Scientific data is collected and displayed in near real time from selected nearby CART sites. This data assists in mission planning and allows the scientists to correlate data from ground instruments, airborne sondes, and satellite images with measurements and observations from the UAV aircraft.

The logging capability promotes the capture of time tagged events which document the mission and facilitate controller process improvement, and mission or data problem identification and correction. The logging system is also connected to the aircraft position and attitude data so that these can be entered directly in real time into the log.

Numerous radios allow the mission controller to maintain constant and reliable contact with pilots, ground crews, payload ground station, safety personnel, and others. In addition, the mission controller has an uplink capability to send commands to individual payload instruments. This uplink allows the instrument mentors to reset, shutdown, restart, etc. their instruments through the mission controller based on payload and instrument status information displayed in real time.

Post-Flight Data Management

Post-flight data management takes the full data set (not subsampled) collected from the onboard aircraft instruments to a complete, well documented data set of known and reasonable quality in a relatively short time frame. A great deal of effort is taken to ensure the quality and usability of this data. Since the equipment, goals, and conditions shift from mission to mission, full, accessible, and careful documentation of each mission, flight, and instrument is essential.

Data Reduction and Value Added

Raw signal data is collected via telemetry in real-time or via tape (post-flight) and stored in preliminary netCDF files by aircraft and data set. These files are written to tapes mailed to the off-site, primary data processing facility along with the mission logs and instrument lists.

The processing system merges information from the three sources (tapes, logs, and lists) to produce the lowest level (a0) releasable data. During this processing, necessary documentation is added, check sums and sync points are checked. Some data is byte swapped; other data is unpacked and repackaged in a more user-friendly format. The value added processing is performed at this stage rather than during the time critical

on-site processing. Figure 37 is a schematic showing the flow of data for each campaign.

The level a0 data is distributed to the instrument mentors for additional value added processing. The instrument mentors provide validation files and derived, higher level (a1,b1) data which is collected by the primary processing facility. The netCDF data files are self-documenting and have considerable information about the data and limited information about the source instrument in the file header. The validation files contain more detailed information about the data, the source instrument, the processing algorithm, calibration factors, and quality check procedures.

Data Release

The scientific data and validation files are gathered at the primary processing facility and stored in a logical directory structure to facilitate access. In addition to the scientific data and validation files, the complete UAV mission data set includes a number of files that document the flights both operationally and scientifically. Such documentation may include the mission experiment plan, a summary of each flight in a mission including the weather conditions and items of scientific note by the Mission Scientist, the full set of Mission Scientist and Mission Controller logs, flight cards, and README files with important notes specific to a mission, flight, air-

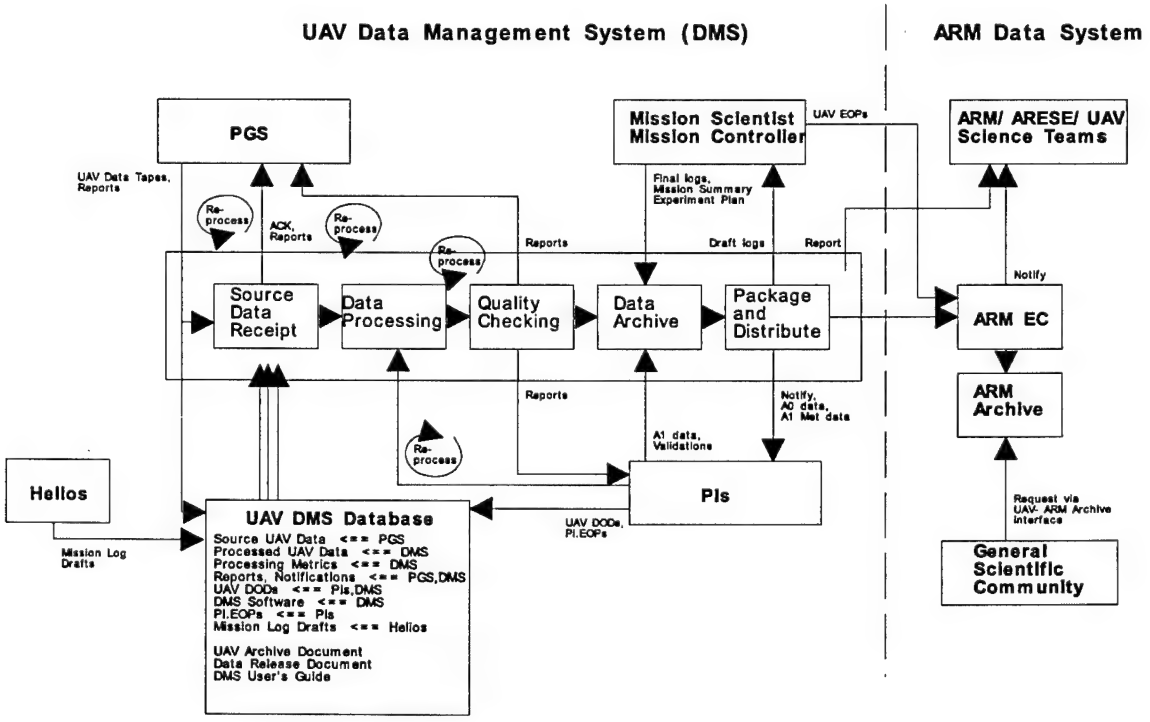

Figure 37. Schematic of the Data Management System.

craft or instrument. A document explaining the directory structure and naming conventions is also provided. In the case where there is collateral data not normally archived by the ARM data system, this is collected, documented and stored with the UAV program data.

Data release meetings are typically held midway and at the end of the data processing period. The first, or "preliminary", meeting is held after the instrument mentors have received all their level a0 data and have completed the validation and level a1 processing for one or two flights. This meeting is a peer review of the data. Topics for discussion include the quality/completeness of the data documentation, the value of the measurements (is anything missing?), and preliminary analysis. This meeting generally results in a fair number of action items for the data processors which are to be resolved before the second and final data release meeting.

During the final data release meeting which is held after all the data has been processed, the issues of the first meeting are revisited and the data further inspected. Questions about correlation are considered. Plans are made for World Wide Web pages to provide a data sampler for potential users.

When the data set is complete, it is transferred to the ARM Archive for access by the general scientific community. The ARM Archive has adequate space and equipment to keep the data accessible for an extended period (~20 years). The ARM Archive has developed a system that allows users to create data requests or "orders" on line via the Internet. These orders are subsequently filled and the user notified to retrieve the data by Internet ftp.

Chapter

6

Transition of Project to the DOE

From it's inception, the intent of this program has been to develop instrumentation and measurement techniques that could be transferred to other agencies - most notably the Department of Energy - for use in their programs targeted at reducing the uncertainty in radiation cloud interactions and hence in greenhouse warming predictions. The Department's Atmospheric Radiation Measurements (ARM) Program contains several highly instrumented ground based sites aimed at improving the understanding of radiation cloud interactions. The data sets collected at these sites will benefit greatly from the addition of data from the UAV borne measurement capabilities we have demonstrated in this program, including the ability to create in effect a "geostationary satellite" at the tropopause centered over these Cloud and Radiation Testbeds (CARTs).

Given the success of the ARSAP program in developing the needed UAV measurement techniques and in contributing to the understanding of radiation cloud interactions, the Department of Energy has agreed to the transition of this program to its own funding structure and to fund it effective FY97. The first campaign following transition is scheduled for the Oklahoma CART site in Fall of 1997. The resulting data will be processed and distributed as part of the ARM data stream. This capability will be factored into all future ARM scientific planning and science team activities.

Chapter

7

Summary

The Atmospheric Remote Sensing and Assessment Program (ARSAP) was jointly conducted by Sandia National Laboratories for the DOE and the Naval Research Laboratory for DOD. Its goal was to develop improved measurements and understanding of the Earth's atmosphere and its response to global change based upon unique DOD and DOE technologies. The DOE role focused on the uncertainties associated with current knowledge of cloud-radiation interactions and how these uncertainties influence our ability to understand the effects of increasing concentrations of greenhouse gases in the atmosphere.

The DOE side of this effort has developed techniques for the measurement of atmospheric heating in a well defined layer and then relating this measurement to the cloud properties and water vapor contained in the layer. This allows the testing and refining of the models that predict atmospheric heating based on such parameters. Succinctly stated, the DOE objective was (1) to develop high accuracy measurements techniques, (2) to use them to make sustained measurements up to the tropopause, and (3) to use these measurements to calibrate existing satellites and their data products to the accuracy required for climate measurements, thereby leveraging this national resource.

It was quickly determined that combined altitude (14 km in the mid latitudes and 20 km in the tropics) and endurance requirements (> 24 hrs on station) are beyond the capability of manned aircraft and are best met using the UAVs that under development by industry. Given this, and drawing on DOE and DOD related defense technology, seven new UAV compatible (compact, lightweight, and capable of fully autonomous operation) instruments were developed to make the kind of atmospheric flux, radiance, and cloud measurement measurements needed and at the accuracy required. The six are (1) the Cloud Detection Lidar, (2) the UAV Atmospheric Emitted Radiance Interferometer, (3) the Hemispheric Optimized Net Radiometer, (4) the Multispectral Pushbroom Imaging Radiometer, (5) the frost point and laser diode hygrometers, and (6) Scanning Spectral Polarimeter. Each is discussed in detail in the main body of this report.

In cooperation with the DOE Atmospheric Radiation Measurement (ARM) program, four major field campaigns were undertaken at the Cloud and

Atmospheric Radiation Testbed (CART) Site in north central Oklahoma to make critically needed atmospheric measurements. During the course of these campaigns techniques for using UAVs in conjunction with manned aircraft were developed while utilizing many of the new instruments. The three to six week campaigns were flown in April 1994, October 1995, April 1996, and September 1996. During each flight of each campaign, data taken by the aircraft were telemetered to the ground for real time analysis by the mission scientist and instrument Principle Investigators (PIs); this analysis often resulted in minor modifications to the planned mission based on atmospheric conditions and instrument performance.

Key scientific results from the field campaigns include the profiling of clear sky fluxes from near surface to 14 km in altitude with unprecedented accuracy and the strong indication of cloudy atmosphere absorption of solar radiation as much as 50% greater than that predicted by the best extant models. These early results were then integrated with related Atmospheric Radiation Measurement (ARM) measurements and Computer Hardware, Applied Mathematics, and Model Physics (CHAMMP) modeling efforts for the development of improved climate models.

Key technical accomplishments include the first ever use of UAVs for atmospheric research, the flight of UAVs in civilian airspace without chase, precision stacked flight with manned aircraft and a UAV maintaining lateral separation of a few hundred meters with vertical separations of 10 km, and a diurnal UAV mission with greater than 24 continuous hours on station without refueling.

Appendix

A

Science Team Projects

1. Cloud and Satellite Instrument Calibration from UAVs; Catherine Gautier; University of California, Santa Barbara.

2. Satellite Calibration and Verification of Remotely Sensed Cloud and Radiation Properties Using ARM UAV Data; Patrick Minnis, Thomas P. Charlock, and Charles H. Whitlock; NASA Langley Research Center.

3. Surface Characterization and Radiation Modeling for Analyzing Upwelling Radiation Measured by Unmanned Aerospace Vehicles and Satellites across the CART Site; Weigang Gao, Richard L. Coulter, and Barry M. Lesht; Argonne National Laboratory.

4. Interpretation of Radiation Measurements from Unmanned Aerospace Vehicles (UAVs); K. N. Liou; University of Utah.

5. Sampling Studies for ARM-UAV Missions; Robert F. Cahalan; NASA Goddard Space Flight Center.

6. Studies of Cloud Radiation Fields; Peter H. Daum; Brookhaven National Laboratory.

7. Direct Measurement of Shortwave Radiative Forcing by Clouds; Stephen E. Schwartz; Brookhaven National Laboratory.

8. Research with Unmanned Aerospace Vehicles, UAV Radiation Measuring System (UAV RAMS); Francisco Valero; Scripps Institution of Oceanography.

9. UAV Applications for Studying the Radiation and Optical Properties of Upper Tropospheric Clouds; Graeme L. Stephens and Stephen K. Cox; Colorado State University.

10. High Spectral Resolution Atmospheric Emitted Radiance Studies with the ARM UAV; Henry E. Revercomb, William L. Smith, and Robert O. Knuteson; University of Wisconsin, Madison.

11. Remote Sensing of Total Water Vapor and Liquid Water and Profiles of Cloud Water Using Microwave Radiometer and Radar Measure-

ments; James A. Weinman, Paul E. Racette, and Warren J. Wiscombe; NASA Goddard Space Flight Center.

12. Development of a UAV Mounted 95 GHz Radar System to Conduct Scientific Studies of Clouds; Robert E. McIntosh; University of Massachusetts.

DISTRIBUTION:

1 Dr. Ralph Alewine
Director of Nuclear Monitoring Division
Defense Advanced Research Projects Agency (DARPA)
1901 N. Moore Street, Suite 609
Arlington, VA 22209

1 Mr. Paul Bourget, Action Officer
(Mr. Grant Aufderhaar, Support)
National Reconnaissance Office
14675 Lee Road
Chantilly, VA 20151-1750

1 Dr. Michelle Broido, Director
Environmental Sciences Division, ER-74
U.S. Department of Energy
19901 Germantown Road
Germantown, MD 20874-1290

1 Dr. Robert F. Cahalan
NASA Goddard Space Flight Center, Code 913
Greenbelt, MD 20771

1 Dr. Ric Cederwall
Atmospheric Science Division (L-103)
Lawrence Livermore National Laboratory
P.O. Box 808
Livermore, CA 94551

1 Dr. Thomas P. Charlock
NASA Langley Research Center
Hampton, VA 23681-0001

1 Defense Technical Information Center (DTIC/OCP)
Attn: Joyce Chiras
8725 John J. Kingman Road
Fort Belvoir, VA 22060-6218

1 Dr. Richard L. Coulter
Building 203, Environmental Research Division
Argonne National Laboratory
9700 S. Cass Ave.
Argonne, IL 60439

1 Dr. Stephen K. Cox
Department of Atmospheric Science
Colorado State University
Ft. Collins, CO 80523-1371

1 Dr. Ted Cress
Pacific Northwest Laboratories
POB 999
Richland, WA 99352

15 Dr. Patrick Crowley, Project Manager
Environmental Sciences Division, ER-74
U.S. Department of Energy
19901 Germantown Road
Germantown, MD 20874-1290

1 Dr. Peter Daum
Environmental Chemistry Division
Brookhaven National Laboratory
Upton, NY 11973-5000

1 Dr. Phillip A. Durkee
Department of Meteorology, Code MR/De
Naval Postraduate School
589 Dyer Road, Room 254
Monterey, CA 93943-5114

3 Dr. Bob Ellingson
Meteorology Department
Computer and Space Science Building
University of Maryland at College Park
College Park, MD 20742

1 Dr. Jerry Elwood (Stephen Herrick)
Program Manager
ER-74 - Germantown Building
U.S. Department of Energy
19901 Germantown Road
Germantown, MD 20874-1290

1 Dr. Wanda R. Ferrell, Data Program Manager
Environmental Sciences Division, ER-74
U.S. Department of Energy
19901 Germantown Road
Germantown, MD 20874-1290

1 Dr. Weigang Gao
Building 203, Environmental Research Division
Argonne National Laboratory
9700 S. Cass Ave.
Argonne, IL 60439

1 Dr. Catherine Gautier
Earth Space Research Group
CRSEO - Ellison Hall
University of California
Santa Barbara, CA 93106

1 Dr. Richard B. Gomez
Associate Director of Technology
U.S. Army Topographic Engineering Center
Building 2592 Attn: CETEC-TD
7701 Telegraph Road
Alexandria, VA 22315-3864

1 Dr. Jorg Hacker
Institute for Atmospheric and Marine Sciences
Flinders University
GPO Box 2100
Adelaide 5001
Australia

2 SERDP Support Office
Attn: Mr. Mike Hathaway
8000 Westpark Drive, Suite 400
McLean, VA 22102

1 Mrs. Susan L. Havre
ARM-UAV Data Management System
Pacific Northwest National Laboratory, K2-78
POB 999
Richland, WA 99352

1 Dr. Don Hunton
Manager of Environmental Research
PL/GPID
29 Randolph Road
Hanscom AFB, MA 01731-3010

1 Dr. David Jasper
BMRC
GPO Box 1289K
Melbourne, Victoria
Australia 3001

1 Dr. Kenneth Johnston, Scientific Director
U.S. Naval Observatory
3450 Massachusetts Avenue, N.W.
Washington, D.C. 20392-5420

1 Dr. Robert O. Knuteson
Space Science and Engineering Center
University of Wisconsin - Madison
1225 W. Dayton St.
Madison, WI 53706

1 Dr. Peter LaDelfe
Los Alamos National Laboratory, NIS-2, MS D436
Los Alamos, NM 87545

1 Dr. Barry M. Lesht
Building 203, Environmental Research Division
Argonne National Laboratory
9700 S. Cass Ave.
Argonne, IL 60439

1 Dr. Kuo-Nan Liou
Department of Meteorology, Rm 819 W. B. B.
University of Utah
Salt Lake City, UT 84112

1 Dr. Peter Lunn
Environmental Sciences Division, ER-74
U.S. Department of Energy
19901 Germantown Road
Germantown, MD 20874-1290

1 Dr. Robert E. McIntosh
Knowles Engineering Building
University of Massachusetts
Amherst, MA 01003

1 Dr. Patrick Minnis
NASA Langley Research Center MS 420
Hampton, VA 23681-0001

1 Dr. Muhammad Owais, Program Manager
Defense Nuclear Agency
Radiation Policy Division
6801 Telegraph Road
Alexandria, VA 22315-3864

1 Dr. Ari Patrinos, Associate Director
Office of Health and Environmental Research (ER-70)
U.S. Department of Energy
19901 Germantown Road
Germantown, MD 20874-1290

1 Dr. Shelly Pope
University of California San Diego
Scripps Institution of Oceanography, Mail Code 0221
La Jolla, CA 92093

1 Dr. Paul E. Racette
Microwave Sensor Branch, Code 975
NASA Goddard Space Flight Center
Greenbelt, MD 20771

1 Dr. Henry E. Revercomb
Space Science and Engineering Center
University of Wisconsin - Madison
1225 W. Dayton St.
Madison, WI 53706

1 Dr. Dan Rodriguez
Atmospheric Science Division (L-103)
Lawrence Livermore National Laboratory
P.O. Box 808
Livermore, CA 94551

1 Dr. Phillip Russell
NASA Ames Research Center
MS 245-5
Moffett Field, CA 94035-1000

1 Dr. Patricia A. Sanders, Director
Test, Systems Engineering, and Evaluation
DT&E, Room 3D1067
3110 Defense Pentagon
Washington, D.C. 20301-3110

1 Dr. Phillip R. Schwartz, Superintendent
Remote Sensing Division (7200)
Naval Research Laboratory
Washington, D.C. 20375-5320

1 Dr. Stephen E. Schwartz
Environmental Chemistry Division
Brookhaven, National Laboratory
Upton, NY 11973

1 Dr. Doug Sisterson
Argonne National Laboratory
Environmental Research Division
9700 S. Cass Avenue, Bldg. 203
Argonne, Illinois 60439

1 Dr. William L. Smith
Space Science and Engineering Center
University of Wisconsin - Madison
1225 W. Dayton St.
Madison, WI 53706

1 Dr. Dave Sowle
Mission Research Corporation
735 State St.
P. O. Drawer 719
Santa Barbara, CA 93102

1 Dr. Graeme Stephens
Department of Atmospheric Science
Colorado State University
Ft. Collins, CO 80523-1371

1 Dr. Gerry Stokes
Pacific Northwest National Laboratory
POB 999
Richland, WA 99352

1 Dr. Dennis A. Trout
Atmospheric Sciences Research Program Manager
National Center for Environmental Assessment (8623)
U.S. Environmental Protection Agency (Mail Drop - M3817I)
401 M Street, S.W.
Washington, D.C. 20460

1 Dr. Paul Try
International GEWEX Project Office
Suite 203
409 Third Street SW
Washington, DC 20024

1 Dr. Francisco Valero
Scripps Institution of Oceanography
University of California
San Diego, CA 92093-0230

1 Dr. Paul Weber
Los Alamos National Laboratory, NIS-2 D436
Los Alamos, NM 87545

1 Dr. Steven Wegener
NASA Ames Research Center
MS 245-5
Moffett Field, CA 94035-1000

1 Dr. James A. Weinman
Microwave Sensor Branch, Code 975
NASA Goddard Space Flight Center
Greenbelt, MD 20771

1 Dr. Charles H. Whitlock
NASA Langley Research Center
Hampton, VA 23681-0001

1 Mr. Roger Wingert
ZKC 4.1
250 S. Rogers Rd
Olathe, KS 66062

1 Dr. Warren J. Wiscombe
Microwave Sensor Branch, Code 913
NASA Goddard Space Flight Center
Greenbelt, MD 20771

1 Dr. Ronald Wurtz
Lawrence Livermore National Laboratory
Mail Stop L-410, 7000 East Avenue
Livermore, California 94550

1	MS 9001	T. O. Hunter; Attn:	MS 9002	P. N. Smith, 8500
			MS 9003	D. L. Crawford, 8900
			MS 9005	J. B. Wright, 2200
			MS 9009	R. C. Wayne, 8400
			MS 9054	W. J. McLean, 8300
			MS 9141	P. E. Brewer, 8800
			MS 9405	T. M. Dyer, 8700
			MS 9420	L. A. West, 8200
5	MS 9104	W. Bolton, 8120		
1	MS 9101	R. Busbee, 8411		
1	MS 9044	M. E. John, 8100		
1	MS 9056	M. Lapp, 8102		
1	MS 0980	G. S. Phipps, 5725		
20	MS 9056	T. Tooman, 8120		
10	MS 9056	J. Vitko, Jr., 8102		
10	MS 9021	Technical Communications Department, 8815 for OSTI		
1	MS 9021	Technical Communications Department, 8815 / Technical Library, MS 0899, 4414		
4	MS 0899	Technical Library, 4414		
3	MS 9018	Central Technical Files, 8940-2		

Org.	Bldg.	Name	Rec'd by	Org.	Bldg.	Name	Rec'd by

LS 2900-QE

Sandia National Laboratories